N22

BNWL-193

105-

AEC RESEARCH and DEVELOPMENT REPORT

PHYSICS RESEARCH QUARTERLY REPORT JULY, AUGUST, SEPTEMBER, 1965

THE STAFFS OF
REACTOR PHYSICS,
EXPERIMENTAL PHYSICS RESEARCH
AND
CRITICAL MASS PHYSICS

OCTOBER 15, 1965

BATTELLE-NORTHWEST
BATTELLE MEMORIAL INSTITUTE / PACIFIC NORTHWEST LABORATORY

LEGAL NOTICE

PACIFIC NORTHWEST LABORATORY
RICHLAND, WASHINGTON
operated by
BATTELLE MEMORIAL INSTITUTE
for the
UNITED STATES ATOMIC ENERGY COMMISSION UNDER CONTRACT AT(45-1)-1830

PRINTED BY/FOR THE U. S. ATOMIC ENERGY COMMISSION

AEC-RLOO RICHLAND, WASH.

N22

BNWL-193
UC-34, Physics

FIRST UNRESTRICTED | TID-4500

DISTRIBUTION MADE | EDITION

PHYSICS RESEARCH QUARTERLY REPORT
JULY, AUGUST, SEPTEMBER, 1965

By

The Staffs of
Reactor Physics,
Experimental Physics Research
and
Critical Mass Physics

F. G. Dawson, Jr.	Manager Reactor Physics
C. W. Lindenmeier	Manager Theoretical Physics
L. C. Schmid	Manager Light Moderator Reactor Physics
P. L. Hofmann	Manager Engineering Physics
H. L. Henry	Manager Experimental Reactors
R. E. Heineman	Manager High Temperature Reactor Physics
D. D. Lanning	Manager Heavy Moderator Reactor Physics
B. R. Leonard, Jr.	Manager Experimental Physics Research
E. D. Clayton	Manager Critical Mass Physics

Physics and Instruments Department

October 15, 1965

PACIFIC NORTHWEST LABORATORY
RICHLAND, WASHINGTON

Printed in USA. Price $3.00. Available from the
Clearinghouse for Federal Scientific and Technical Information
National Bureau of Standards
U.S. Department of Commerce
Springfield, Virginia

TABLE OF CONTENTS

PREVIOUS REPORTS IN THIS SERIES

HW-42181	October, November, December	1955
HW-43441	January, February, March	1956
HW-44525	April, May, June	1956
HW-47012	July, August, September	1956
HW-48893	October, November, December	1956
HW-50598	January, February, March	1957
HW-51983	April, May, June	1957
HW-53492	July, August, September	1957
HW-54591	October, November, December	1957
HW-55879	January, February, March	1958
HW-56191	April, May, June	1958
HW-57861	July, August, September	1958
HW-59126	October, November, December	1958
HW-60220	January, February, March	1959
HW-61181	April, May, June	1959
HW-62727	July, August, September	1959
HW-63576	October, November, December	1959
HW-64866	January, February, March	1960
HW-66215	April, May, June	1960
HW-67219	July, August, September	1960
HW-68389	October, November, December	1960
HW-69475	January, February, March	1961
HW-70716	April, May, June	1961
HW-71747	July, August, September	1961
HW-72586	October, November, December	1961
HW-73116	January, February, March	1962
HW-74190	April, May, June	1962
HW-75228	July, August, September	1962
HW-76128	October, November, December	1962
HW-77311	January, February, March	1963
HW-77871	April, May, June	1963
HW-79054	July, August, September	1963
HW-80020	October, November, December	1963
HW-81659	January, February, March	1964
HW-83187	April, May, June	1964
HW-84369	July, August, September	1964
HW-84608	October, November, December	1964
BNWL-95	January, February, March	1965
BNWL-149	April, May, June	1965

LIGHT MODERATOR REACTOR PHYSICS

Modifications to the Computer Code, Thermos, and Comparative Studies on Scattering Kernels

J. R. Worden, W. L. Purcell, and R. C. Liikala

Introduction

For the past several months, the computer code, THERMOS,[1] has been used extensively at Battelle Northwest Laboratories for calculating the spatial and energy distribution of the neutron flux in unit cells of thermal reactors. During this time it has been found desirable to make certain changes and/or additions to the code that

- reduce the time and effort required to perform calculations using THERMOS,
- increase the flexibility of the code, or
- adapt the code to special problems.

This report summarizes the options available at Battelle-Northwest for calculations using THERMOS. The modifications have proven useful here and are summarized since similar changes may be of use at other laboratories.

The remainder of the report describes the method by which cross section data are obtained and prepared for THERMOS and an extended version of THERMOS available for use on the Univac 1107. Finally, scattering kernels in use for the common moderating materials are described along with a summary of the results of some comparative studies on the effect of of the choice of scattering model on calculated reactor parameters.

THERBAR–Data Tape Preparation

Access to the cross section data of the Battelle Northwest Master Library[2] (formerly the RBU Basic Library)[3] has been provided through a program chain, called THERBAR. This code is basically a chain connecting BARNS,[4] which reads the basic library, LIBP,[1] which prepares a data tape for THERMOS, and THERMOS itself.

The primary incentive for this work was to reduce the time and effort required to perform calculations using THERMOS An important secondary benefit is derived by having easy access to the standard cross section data of the basic library This allows the desirable situation that comparative studies on different systems, perhaps performed by more than one person, may be normalized to the same basic data.

A subroutine, VELCON, is included in the chain for the purpose of converting from group boundary energies, which are input data for the code, to velocities as required by THERMOS. The velocity width and midpoint velocity are required on a THERMOS data tape. The energy corresponding to the midpoint velocity of each group is calculated in VELCON and it is at these energies that cross section are read from the basic library.

Univac 1107 Version

The original version of THERMOS, programmed for an IBM 7090, has been converted to FORTRAN IV, and compiled on the Univac 1107. At the same time, the number of space points available in a calculation has been increased from 20 to 25, and the number of energy groups has been increased from 30 to 40 A data tape is available which has groups over the energy range 0 to 1.3 eV, thus spanning the 1.056 eV resonance in the Pu^{240} cross section. This permits study of the effect of this resonance on the thermal flux shape in reactor cells. For example, the calculated neutron spectrum at the center of a 19-rod cluster of UO_2-2 wt% PuO_2 in D_2O moderator is shown in Figure 1. The plutonium was assumed to contain 8 wt% Pu^{240}. The upper curve of the figure was calculated using the IBM 7090 version of THERMOS with an energy mesh over the range 0 to 0.683 eV. The lower curve was calculated using the Univac 1107 version with 40 energies as described above. The curves are normalized to give the same integrated flux over the energy range 0 to 0.683 eV. As expected, the effect of the Pu^{240} resonance is to deplete the flux over the thermal energy range. In order to demonstrate the importance of the differences in the shape of the two curves, average absorption and fission cross sections are listed on the figure, averaged over each of the two spectra. It is seen that the average cross sections differ by about 4%, although the ratio, absorption to fission, is the same in both cases.

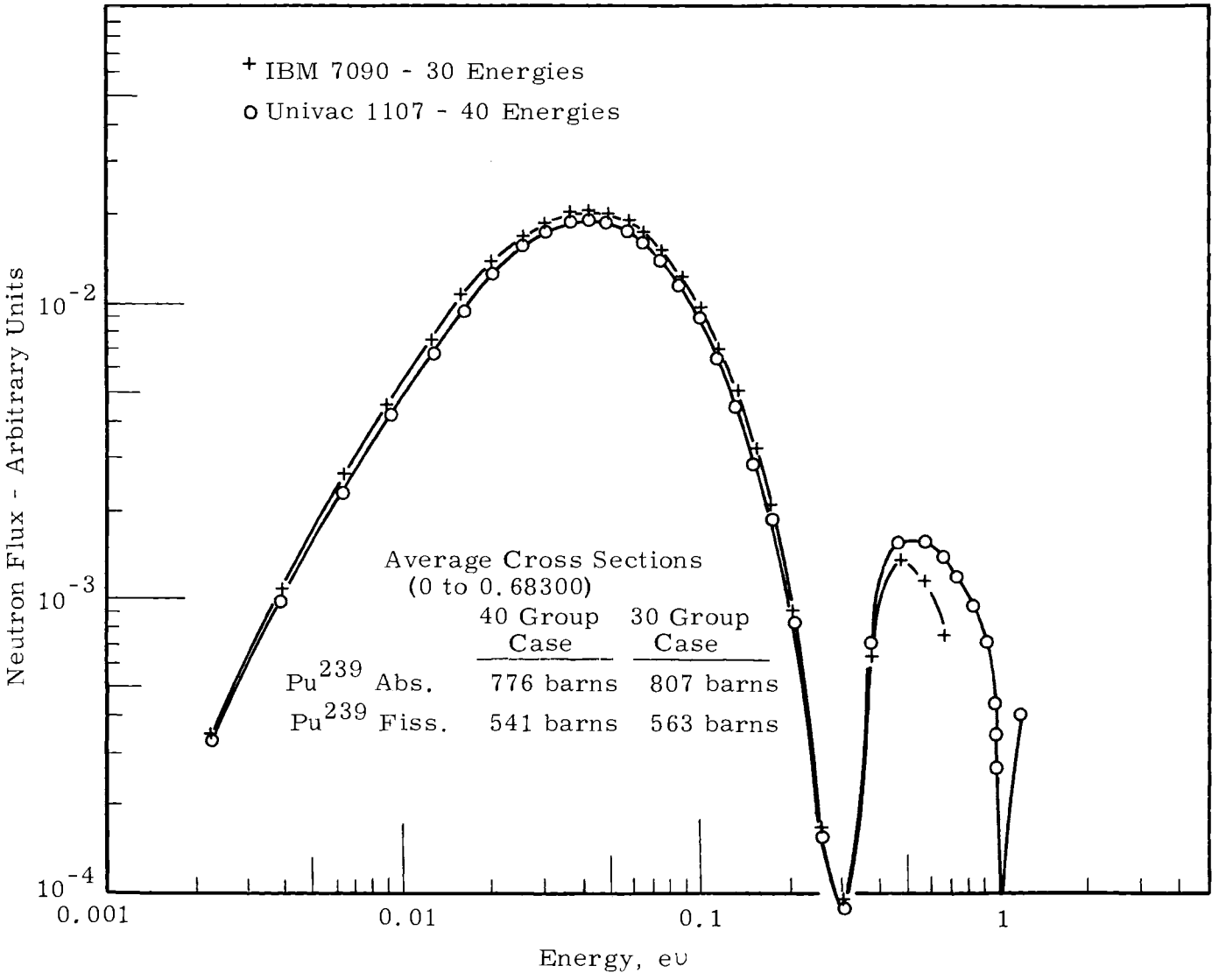

FIGURE 1

Neutron Spectrum at C_t of 19-Rod Cluster
UO_2-2 wt% PuO_2 in D_2O

Scattering Kernels and Comparative Studies

The Brown-St. John form of the free gas scattering model is built into both the library preparation program, LIBP, and THERMOS itself.[1] This model is used at the Laboratory for all materials on the various THERMOS data tapes with the exceptions of H_2O, D_2O, and graphite.

Water

Scattering kernels for both light and heavy water were generated from the Nelkin scattering model for protons bound in water.[5] This was accomplished using the code, GAKER, which, although a separate program, is essentially part of the THERMOS package. For light water, the parameters used as input to GAKER are those listed in the THERMOS document.[1] For heavy water, a revised set of input parameters were obtained based on an adaptation of the Nelkin model to D_2O by Honeck.[6] The input parameters used in GAKER, for D_2O, are listed in Table I. Values in parenthesis are energies in units of 0.0253 eV. Definitions of the various parameters are given in Appendix E of Reference 1.

TABLE I

INPUT TO GAKER FOR D_2O

Constant	$E \leq 0.30$ eV	$E > 0.30$ eV
$1/\lambda$	20.0	3.409
E	0.0253 eV (1.0)	0.0317 eV (1.253)
A	0 1373 eV (5.427)	1.1729 eV (46.36)
B	0.2377 eV (9.395)	21.05 eV (832.0)
ω	0.05 eV (1.976)	0.15 eV (5.929)
β	14.52	7.26
α/β	0.175 eV (6.917)	0.350 eV (13.83)

Comparisons were made between results of calculations using the Brown-St. John and Honeck kernels for D_2O by analysis of three D_2O-moderated systems; one containing natural uranium (UO_2), a second containing plutonium only (PuAl), and a third containing both plutonium and uranium in the form UO_2-2 wt% RhO_2. In each of these systems, the fuel

was in the form of 19-rod clusters arranged in a hexagonal array with a lattice spacing of 8 in. A model of the cluster was employed consisting of concentric rings of fuel, separated by smeared D_2O and cladding and surrounded by D_2O moderator. Values for thermal utilizations, disadvantage factors, and thermal neutron reproduction factors are compared in Table II. From the table it is obvious that the spatial flux shape as represented by the disadvantage factor and thermal utilization, is nearly independent of which scattering kernel is used. The difference in spectral flux shape is reflected in the values of thermal reproduction factor, $\overline{\eta}$, since this parameter depends only on the neutron spectrum in the fuel and not on the spatial distribution of the integrated flux.* Again, there is little reason to choose between the two models since the values of $\overline{\eta}$ agree to within $\frac{1}{2}$%.

TABLE II

VALUES OF THE DISADVANTAGE FACTOR, THERMAL UTILIZATION, AND $\overline{\eta}$ FOR 8 INCH D_2O LATTICES FUELED WITH NATURAL UO_2, 1.8 wt% PuAl, AND 2 wt% PuO_2-UO_2 19-ROD CLUSTERS

	Disadvantage Factors Φ_{mod}/Φ_{fuel}*		Thermal Utilization, f			$\overline{\eta}$		
	Calculated		Nelkin				Calculated Nelkin	
	Nelkin D_2O	Gas	Exp.	D_2O	Gas	Exp.	D_2O	Gas
Natural UO_2	1.793	1.759	0.900	0.931	0.931	1.322 ± 0.021	1.309	1.313
1.8 wt% PuAl	1.777	1.725	---	0.938	0.938		1.774	1.779
2 wt% PuO_2-UO_2	6.336	5.942	---	0.972	0.971		1.775	1.780

* Φ_{fuel} is the average flux in the center rod of the cluster.

Comparing against experimental data, which are available for the UO_2 system,[7] one observes that the value of $\overline{\eta}$ generated using either model agrees with the experimental value within the quoted uncertainty. On the other hand, both over-predict the thermal utilization, f, by $3\frac{1}{2}$%.** One might suspect that this is due, at least in part, to the approximate

*The calculated value of $\overline{\eta}$ is a spatial average over the fuel. The bar denotes an energy average over the range 0 to 0.683 eV.

**Although the definitions of the calculated and measured thermal utilizations, differ slightly, it is shown in Appendix A that this difference leads to negligible differences in numerical value for the systems considered in this report.

nature of the geometric model of the cluster used in the analysis. It will be shown, however, that much better agreement is obtained in graphite lattices, independent of whether the fuel is in the form of solid rods, tube-in-tube, or 19-rod clusters. One thus concludes on the basis of this rather meager comparison, that further improvement in the scattering model for D_2O should be considered.

Graphite

The scattering model for graphite in local use is that of Parks[8] and the kernels, based on this model, were obtained by use of the computer code, SUMMIT.[9] Since this code computes kernels corresponding to inelastic scattering only, those due to elastic scattering were determined such that the total matrix sums to give the measured scattering cross section at each energy.

Detailed studies of two uranium-graphite lattices were made to test the adequacy of the graphite kernels when used in calculations with THERMOS. The first lattice consists of a solid, natural uranium slug, 2.5 in. in diameter, in a graphite lattice with a spacing of 10.5 in. Experimental data for this lattice are available[10] from an experiment in the Physical Constants Testing Reactor (PCTR).[11] Lattice parameters and thermal flux distributions were calculated using both the free gas and Parks kernels and the results compared to the experimentally determined parameters. The flux distributions are shown in Figure 2 and the lattice parameters are listed in Table III. Results of a similar study on a system like the one above but with tube-in-tube fuel geometry are given in Table IV. Experimental results were obtained from experiments conducted in the PCTR for comparison.[10]

The agreement of the results obtained with the Parks kernel with those obtained experimentally are rather striking, especially when compared to the poor agreement obtained with the gas model. For both experiments, values of $\bar{\eta}$ and f are calculated well within the experimental uncertainties with the Parks kernel, whereas the values of f obtained using the gas model in THERMOS differ from the experimentally determined values by $\frac{1}{2}$%.

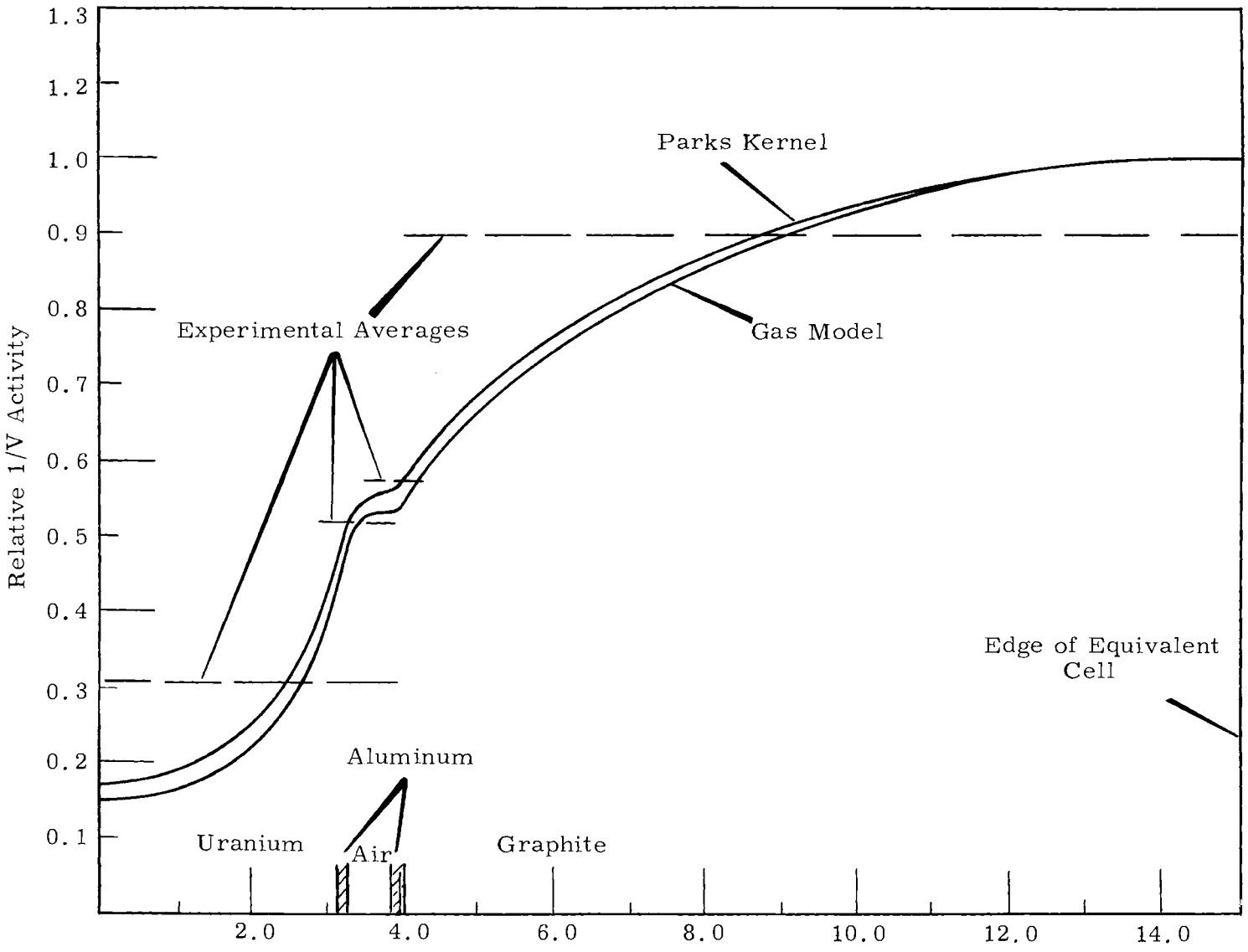

FIGURE 2

Radial Flux Distribution for 2.5 in. Solid Natural Uranium Fueled, 10.5 in. Graphite Lattice, Air Cooled

TABLE III

VALUES OF f AND RELATIVE AVERAGE FLUXES FOR SOLID FUELED GRAPHITE LATTICE, AIR COOLED

	Utilization			Average Fluxes		
		Calculated			Calculated	
Region	Experiment	Gas Model	Summit	Experiment	Gas Model	Summit
Fuel	0.941 ± 0.022	0.930	0.941	0.308	0.265	0.299
Clad	0.004	0.004	0.004	0.520	0.482	0.506
Coolant Tube	0.008	0.006	0.006	0.570	0.539	0.565
Graphite	0.047	0.060	0.049	0.898	0.915	0.919

VALUES OF DISADVANTAGE FACTORS AND $\bar{\eta}$

Disadvantage Factor, Φ_m/Φ_f			$\bar{\eta}$		
	Calculated			Calculated	
Experiment	Gas Model	Summit	Experiment	Gas Model	Summit
2.916	3.453	3.074	1.289 ± 0.013	1.299	1.290

TABLE IV

VALUES OF THERMAL UTILIZATION, DISADVANTAGE FACTOR, AND $\bar{\eta}$ FOR CONCENTRIC TUBE, NATURAL URANIUM, GRAPHITE LATTICE, AIR COOLED

	Disadvantage Factor, Φ_m/Φ_f		Thermal Utilization, f	$\bar{\eta}$
	Inner Tube	Outer Tube		
Experiment	2.592	2.016	0.923 ± 0.003	1.304 ± 0.014
Calculated				
Gas	2.788	2.190	0.909	1.307
Summit	2.569	2.058	0.922	1.297

Similar results have been obtained for the case of a 19-rod cluster of PuO_2-UO_2 in graphite.[12] The ratio of fissions in plutonium and uranium foils at various positions in the cell are summarized in Table V. Again, the results calculated using the Parks kernel are well within the experimental uncertainty as opposed to the results using the gas kernel. As indicated earlier, in the section on D_2O moderated systems, the cylindrical model of the 19-rod cluster is the same in both cases, yet for this graphite lattice, excellent agreement is obtained between calculated and measured parameters when the Park's kernel is used. Furthermore, the agreement is good for a solid rod in graphite where one would not expect any problems to be introduced because of geometry. Thus, it is concluded that the geometrical model of the cluster is adequate and that the differences observed in the D_2O system do indeed reflect inadequacy of the scattering kernels for heavy water.

TABLE V

FISSION CROSS SECTION RATIOS FOR A 0.9 wt% PuO_2 in UO_2
19 ROD CLUSTER IN AN $8\frac{3}{8}$ INCH GRAPHITE LATTICE, AIR COOLED

	Pu to U Fission Cross Section Ratio,			Thermal Utilization		
		Calculated			Calculated	
Radial Position	Experiment	Gas	Summit	Experiment	Gas	Summit
Center Fuel Rod	1.86 ± 0.04	1.70	1.83	0.968 ± 0.002	0.959	0.965
Fuel Ring 1	1.87 ± 0.04	1.72	1.86			
Fuel Ring 2	1.96 ± 0.04	1.76	1.93			
Cell Boundary	2.01 ± 0.04	1.82	2.08			

Conclusions from the Comparative Studies

From the results presented, it is concluded that scattering in graphite is adequately represented by the Park's kernel if the criterion for adequacy is matching the core parameters, $\bar{\eta}$ and f. This has been confirmed for systems containing uranium only and both uranium and plutonium, where, in each case studied, nearly all the calculated values of the parameters agree with those measured within the experimental uncertainty.

The study on D_2O systems, although limited, indicates the need for an improved scattering model for deuterium bound in heavy water. The use of the Brown-St. John modified gas model or the modified Nelkin model will not result in significant differences between calculated values of $\overline{\eta}$ and f, but the discrepancy between calculations, using either model, and measured parameters is $3\frac{1}{2}\%$ in f and about 1% in $\overline{\eta}$ for a natural uranium-D_2O system. Even larger discrepancies are possible in plutonium systems where, typically, the fuel is blacker and the ratio of neutron captures to fission varies more strongly with energy than in uranium systems.

Additional studies are planned to investigate further the adequacy of scattering models for calculations of thermal reactor parameters.

ACKNOWLEDGEMENT

The authors acknowledge the technical assistance of Dr. C. W. Lindenmeier in adapting the scattering kernels for D_2O and graphite. Also, the authors are grateful to Dr. L. D. Schmid for providing measured values of the thermal utilization, previously unpublished, for the mixed oxide cluster in graphite.

REFERENCES

1. H. C. Honeck. THERMOS A Thermalization Transport Theory Code For Reactor Lattice Calculations, BNWL-5826.

2. K. B. Stewart and J. L. Carter, Jr. Battelle-Northwest Master Library, BNWL-CC-325.

3. R. C. Liikala. Updated RBU Basic Library, Volumes 1, 2, 3, HW-75716 and Data and Methods Employed in Updating the RBU Basic Library, HW-75715 (General Electric Company, Richland, Washington).

4. J. L. Carter, Jr. Unpublished data.

5. M. Nelkin. "Scattering of Slow Neutrons by Water," Phys. Rev., vol. 119, pp. 741-746. 1960.

6. H. C. Honeck. "An Incoherent Thermal Scattering Model for Heavy Water," Trans. Am. Nuc. Soc., vol. 5, no. 1. 1962.

7. J. R. Lilley. Correlation of Data on Heavy Water Moderator Cluster Lattices, HW-60275 (General Electric Company, Richland, Washington). May 19, 1959.

8. N. F. Wigner, G. D. Joanou, and D. E. Parks. Neutron Thermalization in Graphite, GA-4169 (General Atomic Division, General Dynamics Corporation), July 5, 1953, also N.S.E. 19, pp. 108-129. 1964.

9. J. Bell. SUMMIT An IBM-7090 Program for the Computation of Crystalling Scattering Kernels, GA-2492 (General Atomic Division, General Dynamics Corporation). February 1, 1962.

10. D. E. Wood, K. R. Birney, and E. Z. Block. "Lattice Parameter Measurements for Solid and Concentric Tubes ofUranium Fuel in Graphite Lattices," N.S.E., vol. 18, pp. 116-125. 1964.

11. R. E. Heineman. "Experience in the Use of the Physical Constants Testing Reactor," Proceedings of Conference on the Peaceful Uses of Atomic Energy, vol. 12, p. 1929. September, 1958.

12. T. B. Thornbury and N. A. Hill. Unpublished Data.

APPENDIX A

CORRESPONDENCE BETWEEN CALCULATED AND MEASURED THERMAL UTILIZATIONS

The thermal utilization, as usually derived[11] from measured quantities, is defined by

$$f = \frac{\int_0^{E_c} \Sigma_a^{fuel}(E)\,\bar{\Phi}(E)dE + \Sigma_a^{fuel}(E_o)\int_{E_c}^{\infty}\sqrt{\frac{E_o}{E}}\,\bar{\Phi}(E)dE}{\int_0^{E_c} \Sigma_a^{cell}(E)\,\bar{\Phi}(E)dE + \Sigma_a^{cell}(E_o)\int_{E_c}^{\infty}\sqrt{\frac{E_o}{E}}\,\bar{\Phi}(E)dE} \quad . \quad (1)$$

The parameter, E_c, is the effective cadmium cut-off energy, Σ_a^{cell} and Σ_a^{fuel} are the total effective cross section of all materials in the cell and fuel respectively. For simplicity, the spatial dependence of the neutron flux, $\bar{\Phi}(E)$, has been suppressed. This does not affect the conclusions to follow since the equation can be considered as applying to a smeared equivalent of the heterogeneous cell.

From a thermalization code, such as THERMOS, one attains,

$$f' = \frac{\int_0^{E_c} \Sigma_a^{fuel}(E)\,\bar{\Phi}(E)dE}{\int_0^{E_c} \Sigma_a^{cell}(E)\,\bar{\Phi}(E)dE} \quad . \quad (2)$$

Thus, in order to compare the calculated value, f', to the measured value, f, a correction must be made for epi-cadmium, 1/v, absorptions in all the various components of the cell. It is the purpose here to derive an expression relating f and f'.

For convenience, consider the parameters, g and g', defined by

$$g = \frac{1}{f} - 1$$

and

$$g' = \frac{1}{f'} - 1 \quad . \tag{3}$$

From Equation (1), it can be shown that

$$g = \frac{\int_0^{E_c} \Sigma_a^{NF}(E)\Phi(E)dE + \Sigma_a^{NF}(E_o)\int_{E_c}^{\infty}\sqrt{\frac{E_o}{E}}\,\Phi(E)dE}{\int_0^{E_c} \Sigma_a^{F}(E)\Phi(E)dE + \Sigma_a^{F}(E_o)\int_{E_c}^{\infty}\sqrt{\frac{E_o}{E}}\,\Phi(E)dE} \tag{4}$$

where the superscript NF denotes nonfuel materials in the cell only, and F denotes fuel.

Similarly, from Equation (2),

$$g' = \frac{\int_0^{E_c} \Sigma_a^{NF}(E)\Phi(E)dE}{\int_0^{E_c} \Sigma_a^{NF}(E)\Phi(E)dE} \quad . \tag{5}$$

Rewriting Equation (4) and substituting Equation (5),

$$g = \frac{\int_0^{E_c} \Sigma_a^{NF}(E)\,\Phi(E)\,dE}{\int_0^{E_c} \Sigma_a^{F}(E)\,\Phi(E)\,dE} \left[\frac{1 + \dfrac{\Sigma_a^{NF}(E_o) \displaystyle\int_{E_c}^{\infty} \sqrt{\frac{E_o}{E}}\,\Phi(E)\,dE}{\displaystyle\int_0^{E_c} \Sigma_a^{NF}(E)\,\Phi(E)\,dE}}{1 + \dfrac{\Sigma_a^{F}(E_o) \displaystyle\int_{E_c}^{\infty} \sqrt{\frac{E_o}{E}}\,\Phi(E)\,dE}{\displaystyle\int_0^{E_c} \Sigma_a^{F}(E)\,\Phi(E)\,dE}} \right] \tag{6}$$

or

$$g = \gamma g' \tag{7}$$

since the term outside the brackets in Equation (6) is g', from Equation (5), and the term inside the brackets is defined as γ. If Equation (7) is rewritten in terms of f and f' from Equation (3), it can be shown that

$$f = \frac{f'}{1 - (1 - \gamma)(1 - f')} \tag{8}$$

Equation (8) is the relationship between calculated and measured thermal utilizations. From this equation it is concluded that the smaller the value of f', the larger the difference between f and f'. Also, if the parameter, γ, approaches unity, the numerical value of f' approaches f. It is necessary, therefore, to evaluate the parameter, γ.

A cadmium ratio, as measured with a 1/v detector, is defined by

$$CdR = \frac{\displaystyle\int_0^{E_c} \Phi(E)\,\frac{dE}{E} + \int_{E_c}^{\infty} \Phi(E)\,\frac{dE}{\sqrt{E}}}{\displaystyle\int_{E_c}^{\infty} \Phi(E)\,\frac{dE}{\sqrt{E}}}$$

Rearranging,

$$\frac{1}{CdR - 1} = \frac{\int_{E_c}^{\infty} \Phi(E) \frac{dE}{\sqrt{E}}}{\int_{o}^{E_c} \Phi(E) \frac{dE}{\sqrt{E}}} \quad . \tag{9}$$

If it is assumed that the cross sections of all nonfuel materials in the cell vary as $1/v$ in the thermal region, the quantity on the right of Equation (9) is the same as the ratio of integrals appearing in the numerator of γ, as defined in Equation (6). Now consider the integrals in the denominator,

$$\frac{\Sigma_a^F(E_o)\int_{E_c}^{\infty}\sqrt{\frac{E_o}{E}}\,\Phi(E)dE}{\int_o^{E_c}\Sigma_a^F(E)\,\Phi(E)dE} = \frac{\Sigma_a(E_o)\int_o^{E_c}\sqrt{\frac{E_o}{E}}\,\Phi(E)dE}{\int_o^{E_c}\Sigma_a^F(E)\,\Phi(E)dE} \cdot \frac{\Sigma_a^F(E_o)\int_{E_c}^{\infty}\sqrt{\frac{E_o}{E}}\,\Phi(E)dE}{\Sigma_a^F(E_o)\int_o^{E_c}\sqrt{\frac{E_o}{E}}\,\Phi(E)dE}$$

$$= \frac{\bar{\Sigma}_{1/v}^F}{\bar{\Sigma}^F} \quad \frac{1}{CdR - 1} \tag{10}$$

where $\bar{\Sigma}_{1/v}^F \bar{\Sigma}^F$ is the ratio of the average cross section of the fuel, if it varied as $1/v$, to the actual average value of the fuel cross section. Using the relations given by Equations (9) and (10), one can write,

$$\gamma = \frac{1 + \frac{1}{CdR - 1}}{1 + \frac{\bar{\Sigma}_{1/v}^F}{\bar{\Sigma}^F}\left(\frac{1}{CdR - 1}\right)} \tag{11}$$

The parameter, γ, approaches unity if the CdR is very large, or if all components of the cell, including the fuel, have 1/v cross section dependence on energy in the thermal region.

For most well thermalized systems, it can be deduced that there is little distinction between the numerical values of f and f'. For example, assume that,

$$CdR = 11$$

$$\frac{\bar{\Sigma}^F_{1/v}}{\bar{\Sigma}^F} = 0.80$$

and

$$f' = 0.90.$$

These values represent a more extreme case than any of the systems considered in the main text. From Equation (11),

$$\gamma = \frac{1 + 0.1}{1 + (0.8)(0.1)}$$

$$= 1.018,$$

and from Equation (8),

$$f = \frac{f'}{1 - (1 - 1.018)(1 - 0.90)}$$

or

$$f = \frac{f'}{1.002} \quad .$$

Thus, it is concluded that for the systems considered in the main text, the correction is less than 0.2%, which is smaller than the experimental uncertainties. Therefore, no corrections were made to any of the calculated values of thermal utilization in order to compare to experimental values.

HEAVY MODERATOR REACTOR PHYSICS

PCTR Operational Techniques
Estimation of Expected Experimental Precision

D. D. Lanning and R. E. Heineman

The design of a new experiment for the PCTR[1] should include some estimate of the experimental uncertainty. By utilizing the previous experience of k_∞ measurements with the PCTR it is possible to make a good preliminary estimate of the experimental uncertainty and thus determine an important required quantity for the decision of whether a given experiment is worth the effort. The following outlines a procedure for making the desired estimate.

Experience has shown that a given PCTR reactivity measurement can be produced to ±0.04¢ if the moving face has been opened and then closed, or ±0.02¢ if the measurement is made without moving the face. These uncertainties include the normal corrections for pressure, temperature, and the standard period measurement technique of several continuous time measurements during a single period measurement.

A typical example of a k_∞ measurement can be used to relate the reactivity uncertainties to the expected uncertainty in k_∞ measurement. For the case of a lattice of 19 rod clusters of $\frac{1}{2}$ in. diameter natural uranium oxide rods, it was found that $k_\infty - 1 = 0.06$; it took 300 g of copper in the central cell to poison the lattice to $k_\infty = 1.00$; and the reactivity worth of the copper in the cell was measured to be 30 g copper/¢. Thus in this case, the uncertainty in k_∞ due to the uncertainty in the reproducibility of the measurements becomes (for the face moved measurements)

$$E_{k_\infty}\Big]_{\text{reproducibility}} = \frac{(0.04\sqrt{2})\text{¢}(30\ \text{g/¢})}{300\ \text{g}}\ (0.06),$$

where $0.04\sqrt{2}$¢ is the reactivity uncertainty due to the measurement in a reactivity <u>change</u> which involves two measurements of the reactivity.

The numerical value of E becomes

$$E_{k_\infty}\Big]_{\text{reproducibility}} = \pm 3.4(10)^{-4} = 0.34 \text{ mk}$$

It is important to note that this typical value is insensitive to the position of the copper in the cell since at some other position both the sensitivity and the mass of copper for $k_\infty = 1.0$ will change. Hence, the ratio (30 g/¢ to 300 g) is a constant. Further, it has been found that the worth of copper in k_∞ measurements varies from roughly 20 g/¢ to 50 g/¢ over a wide range of experiments, hence the value of: $\frac{(0.06\ \Delta k)\ 30\ g/¢}{300\ g} = 6$ mk/¢ per 19 rod cluster, is a good estimate for the average sensitivity of the PCTR in terms of measured mk of k_∞/¢ of reactivity.

However, it must be remembered that the sensitivity is dependent on the size of the removable cell and the mass of the fuel in the cell. For example, if one is interested in measuring k_∞ of a single $\frac{1}{2}$ in. diameter rod, instead of the 19 rod cluster with the face remaining closed, the reproducibility for one measurement becomes approximately:

$$E\Big]_{\text{reproducibility}} = 0.34\left(\frac{19}{1}\right)\left(\frac{0.02¢}{0.04¢}\right) = \pm 3.2 \text{ mk},$$

and if the measurement is repeated six times

$$E = \frac{3.2}{\sqrt{6}} = \pm 1.3 \text{ mk}.$$

In this case the sensitivity is estimated to be:

$$0.06\,\frac{19}{1}\,\frac{30\ g/¢}{300\ g} \simeq 110 \text{ mk/¢}.$$

Therefore a more useful number might be derived by including the weight and microscopic absorption cross section of the fuel which for the 19 rod cluster is 11 kg of UO_2 and 7.7 barns or ~85 barns-kg, so that the sensitivity becomes

$$0.06\ \frac{30}{300}\,(85) = 500\ \frac{\text{mk barn-kg}}{¢}$$

The total uncertainty in the measured value of Δk_∞ includes (but is not limited to) a combination of the uncertainty due to the reactivity reproducibility; the uncertainty due to neutron spectral mismatch

conditions; and the uncertainty due to the product of the measured relative flux distributions and macroscopic neutron cross sections.

An estimate can also be made of the expected uncertainty due to mismatch conditions by using the two group theory expression:

$$E_{Mismatch} \simeq \frac{\Delta\phi}{\phi} \frac{\Delta m}{m} .$$

A measure of $\Delta\phi/\phi$ is given by the cadmium ratio matching condition. The uncertainties in the matched condition depend on the accuracy of the cadmium ratio values and the sensitivity of the matching technique; by experience, cadmium ratios are measured within an uncertainty of about ± 0.7% and the matching condition, which involves the comparison of several different cadmium ratio values, is usually determined with a ± 2% uncertainty. To evaluate the mismatch in the adjoint function ($\Delta m/m$) a two group theory result can be used which gives $\frac{m_1}{m_2} \simeq (p - 0.03)$ for a full lattice loading. Since $\frac{m_1}{m_2} \equiv p$ for an infinite lattice and since p is almost always in the range of 0.8 to 1.0, then, it is seen that the fractional mismatch in $\frac{m_1}{m_2}$ is always small, and at most is $\sim 0.05/1 = \pm 0.05$. These values for $\Delta\phi/\phi$ and $\Delta m/m$ give

$$E_{Mismatch} \simeq (0.02)(0.05) = \pm 1.0 \text{ mk},$$

and past experience with the PCTR has indicated that the uncertainty in k_∞ due to the uncertainty in the spectral matching is indeed in the range of 1 to 2 mk. It can be noted that matching the cadmium ratio of gold is not always a sufficient criteria for assuming that the neutron spectrum is matched and the possible mismatch at neutron energies above the gold neutron absorption resonance is a source of further uncertainty.

Finally, the uncertainty in the neutron absorption rates as derived from foil activations, material weights, and neutron cross sections usually results in an uncertainty of about ± 3% of $(k_\infty - 1)$ for uranium lattices. For $(k_\infty - 1) = 0.06$ this uncertainty becomes about ± 2 mk. Notice however, for $(k_\infty - 1)$ values greater than 0.1 this "cross section" uncertainty becomes the dominating uncertainty. Hence the minimum uncertainty for the measurement of k_∞ of a given sized sample occurs when $k_\infty - 1$ is zero.

A few observations can be considered from these uncertainty estimates. First, if the relative change in k_∞ is of interest for two nearly similar samples (such as mixed oxide fuel rods with differing oxide particles) then the cross section and mismatch uncertainties will nearly cancel in the ratio leaving mainly the reproducibility uncertainty. Second, as noted already, the most accurate measurements for the PCTR technique are on samples whose k_∞ is close to unity. Whenever possible it may be best to consider simple geometries for adding neutron poisons to the sample so that the poisoned sample results can be easily compared with calculational techniques. Third, the spectral matching uncertainty gives a base point uncertainty for all k_∞ measurements, in general of the order of ± 1.0 mk. This base can be used as a guide for determining the sample size for the central removable section. That is, the removable section need not be so large that the reproducibility error is a few hundreths of a mk since the uncertainty is already limited to 1 or 2 mk. Fourth, there may be some optimum for core loading and sensitivity balance. The larger the core and buffer loading the better the neutron spectrum may be matched but the lower will be the reactor sensitivity to changes in the central cell. Hence, at some point the loss in sensitivity will cause the reproducibility error to become so large that further spectral matching becomes of secondary importance.

Reactivity Uncertainty Caused by Inhour Equation Parameters

N. A. Hill

Introduction

Reactivity measurements with the PCTR require converting directly measured period data to corresponding reactivity data. Tables of reactivity versus periods which are used for this conversion have been generated for various combinations of delayed fraction β and the prompt lifetime ℓ with the IBM-7090 program "Period-Reactivity." Some examples of these reactivities are shown in Figure 1.

The quantity of interest when measuring k_∞ of a test lattice in the PCTR is the ratio of the central cell worth to the worth of copper poison in the cell. Each worth determination requires at least two reactivity measurements. The worth determinations are usually independent and can be

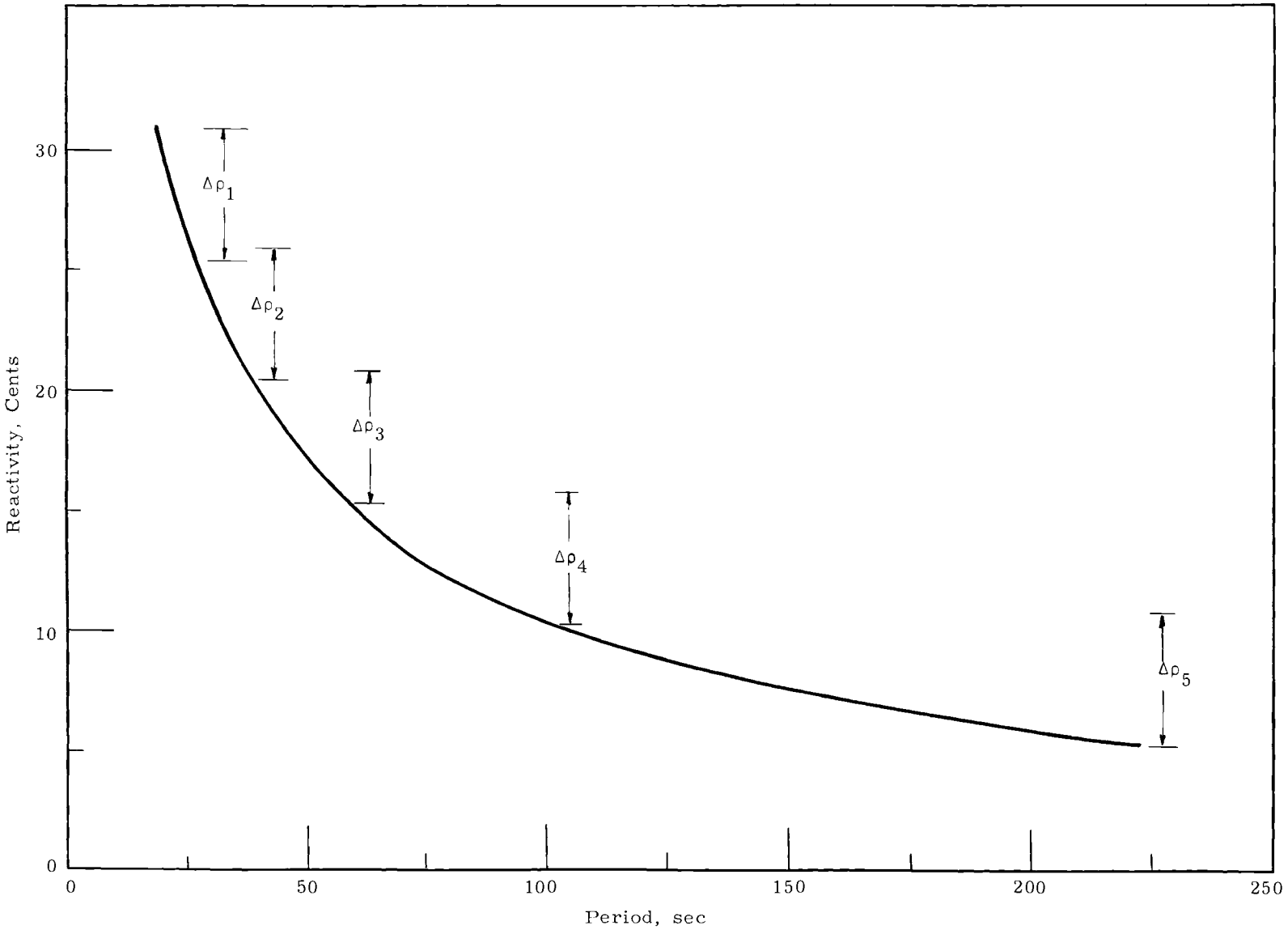

FIGURE 1

Period Versus Reactivity for $\beta = 0.0053$ and $\ell = 0.001$ Seconds

taken in the same general range of periods which minimizes the errors introduced by not knowing the exact constants β and ℓ for each loading. If the worths were measured at widely differing intervals on the period-reactivity curve, a question would arise as to the magnitude of the error introduced into the ratio due to the uncertainty in the reactor constants β and ℓ.

This report describes an experiment designed to measure the reactivity worth of an absorber throughout the useful range of periods from 19 to 222 sec. Analysis of the period data with period-reactivity tables that use different combinations of β and ℓ gives information about the dependence of the reactivity worth of the absorber on the choice of β and ℓ and on the interval at which the worth is measured on the period reactivity curve.

Description of Experiment

The absorber used in the experiment was 0.400 in. of control rod Number 5 in the PCTR from 2.400 to 2.000 in. open out of a full travel of 0.000 to 4.166 in. The base period from which the worth was measured was changed by moving control rod Number 1, the rod furthest from rod Number 5. Table I includes the control rod positions for each period measurement, the corresponding reactivities for three combinations of β and ℓ and the corrections for temperature and pressure variations during the measurements. The pressure and temperature coefficients used were - 0.053¢/mb and - 0.45¢/°C, respectively.

The reactor was fueled with approximately 8.1 kg U^{235} in the core and 5.8 kg U^{235} in the reflectors. The test cavity contained approximately 64.5 kg Th^{232} and 1.25 kg Pu^{239}.

Analysis

Table II includes the measured worth of the absorber for five intervals on the period reactivity curve and for three combinations of β and ℓ. Assuming the reactivity effect of the absorber to be constant, the correct set of tables would lead to a measured worth which would be independent of the interval on the curve over which it was measured.

TABLE I

MEASURED PERIODS AND REACTIVITIES

$\Delta\rho_i$	Period, sec	Rod #	Position, in.	Reactivity ρ β=0.0053 ℓ=0.001 ¢	ρ β=0.0053 ℓ=0.0015 ¢	ρ β=0.0064 ℓ=0.001 ¢	$\Delta\rho_{pressure}$, mb.	$\Delta\rho_{temperature}$, °C
	19.108	5 1	2.4 3.52	30.437	30.929	29.989	+0.138	+0.061
$\Delta\rho_2$								
	26.981	5 1	2.00 3.52	25.057	25.406	24.679	+0.138	+0.065
	26.011	5 1	2.4 3.2	25.600	25.962	25.215	+0.131	0
$\Delta\rho_2$								
	38.365	5 1	2.0 3.2	20.184	20.429	19.872	+0.135	+0.005
	37.207	5 1	2.4 2.880	20.583	20.836	20.265	+0.138	+0.009
$\Delta\rho_3$								
	58.594	5 1	2.0 2.880	15.174	15.334	14.936	+0.138	+0.014
	56.288	5 1	2.4 2.560	15.608	15.775	15.363	+0.138	+0.019
$\Delta\rho_4$								
	100.254	5 1	2.0 2.560	10.163	10.257	10.003	+0.143	+0.024
	94.055	5 1	2.4 2.240	10.682	10.781	10.518	+0.148	+0.041
$\Delta\rho_5$								
	222.320	5 1	2.0 2.240	5.231	5.273	5.150	+0.138	+0.053

TABLE II

CALCULATED WORTH OF ABSORBER

Constants	$\Delta\rho_1(¢)$	$\Delta\rho_2(¢)$	$\Delta\rho_3(¢)$	$\Delta\rho_4(¢)$	$\Delta\rho_5(¢)$	$\Delta\bar{\rho}(¢)$
β=0.053 ℓ=0.001	5.376	5.407	5.404	5.435	5.449	5.414±0.013
$\Delta\rho_i - \Delta\bar{\rho}$	-0.038	-0.007	-0.010	+0.021	+0.035	
β=0.0053 ℓ=0.0015	5.519	5.524	5.497	5.508	5.506	5.511±0.013
$\Delta\rho_i - \Delta\bar{\rho}$	+0.008	+0.013	-0.014	-0.003	-0.005	
β=0.0064 ℓ=0.001	5.306	5.334	5.324	5.350	5.366	5.336±0.013
$\Delta\rho_i - \Delta\bar{\rho}$	-0.030	-0.002	-0.012	+0.014	+0.030	

All the measurements were made without opening the moving face. Previous experience has shown that such reactivity measurements result in an uncertainty of ± 0.02¢ on each measurement leading to an uncertainty of 0.028¢ (or 0.52%) on each change in reactivity (i.e. 5.4¢) worth measurement. Therefore, the expected uncertainty on a ratio of two 5.4¢ worths is 0.74% and the uncertainty on the average of five measurements is ± 0.013¢.

Comparison of the ratios $\Delta\rho_1/\Delta\rho_5$ for the three combinations of β and ℓ show that changing β from 0.0053 to 0.0064 with ℓ = 0.001 sec changes the ratio 0.2% which is well within the experimental uncertainty. Changing ℓ from 0.001 sec to 0.0015 sec with β = 0.0053 causes a change of 1.6% in $\Delta\rho_1/\Delta\rho_5$.

The combination of β = 0.0053 and ℓ = 0.0015 leads to the most consistent set of worth determinations and is the best table to use for this particular reactor loading.

Conclusions

The ratio of reactivity worth measurements is quite insensitive to the value of the delayed fraction β. However, when the prompt lifetime is changed from 0.001 sec to 0.0015 sec, the ratio of worths measured on extreme ends of the useable range for the period-reactivity curve changes more than twice the experimental uncertainty. A method of determining

the correct value of the neutron lifetime to use for a given reactor loading is to repeat this experiment. That is, to determine the combination of β and ℓ which gives the same worth (within the experimental uncertainty) independent of theinterval on the period reactivity curve. The values so determined for the present loading are $\beta \sim 0.006$ and $\ell = 0.0015$ sec.

Reference

1. D. J. Donahue, et al. "Determination of k_∞ from Critical Experiments with the PCTR, Nucl. Sci. Eng., vol. 4, pp. 297-321. 1958.

CRITICAL MASS PHYSICS

Nuclear Criticality Safety Study of FFTF Fuel

C. L. Brown

Critical parameters have been calculated for moderated and unmoderated FTR driver fuel to provide criticality safety guidance for the conceptual design of FFTF examination and storage facilities. These calculations are not intended to constitute a final, rigorous evaluation of the FFTF facilities or nuclear safety practices, but rather to be a quantitative guide for planning and design. The calculated critical parameters are the best estimates of criticality conditions and do not incorporate internal safety factors except as theinherent conservatism of the GAMTEC II program provides.

Aside from considerations of subassembly arrays, nuclear safety in operations involving subassemblies depends strongly on keeping the pins unmoderated. For example, one FTR subassembly represents only 1/100 of a critical mass in air, and 1/6 of a critical mass in water; however, if broken apart in water, the fuel pins of one subassembly represent 2.4 critical masses. Accidental breakage or separation of the fuel pins in subassemblies when under water must be avoided and operations involving the disassembly of subassemblies in water will require rigid controls. Similar controls must also be applied to dry operations that could accidentally be flooded with water. The use of neutron poisons, nonhydrogeneous liquids, or partial disassembly to form subcritical pin bundles prior to transfer to water may somewhat alleviate this problem.

It may be possible to improve criticality safety substantially, regardless of moderation, by adding gadolinium to the stainless steel in the cermet. For example, austentitic stainless steels containing 0.6% gadolinium have been commercially made and the incorporation of 0.5% gadolinium in FTR fuel pins is estimated to increase the initial weighted thermal absorption cross section from 3 to about 280 barns, which would have a significant effect on the critical parameters. Calculations of burnout during reactor operations and the effect of the poison on the FTR would have to be performed to determine whether this addition would be practical.

Methods of Criticality Calculation

Critical parameters were calculated using GAMTEC II,[1] HFN,[2] and Monte Carlo.

GAMTEC II generates multigroup constants for use in the HFN multigroup diffusion theory code. These codes have been under development for several months and have proven to be quite successful for homogeneous plutonium-water systems, and reasonably successful, though conservative, for heterogeneous uranium-water systems. Correlations with experimental measurements have been good and it is believed that GAMTEC II and HFN will be adequately reliable for criticality safety calculations involving FTR fuel (heterogeneous mixtures of plutonium, iron, and water). Nonetheless, it is recognized that without at least one criticality measurement as a check point, a degree of uncertainty must be assumed in the calculations. Future phases of the FFTF program should include one or more criticality experiments to validate the results presented in this study.

Monte Carlo was used to obtain critical parameters for unmoderated FTR fuel. As a confirmation on the results, HFN calculations were also made for the unmoderated system. Critical dimensions from Monte Carlo proved to be about 6% lower than HFN, which is considered to be reasonably good agreement.

The description of the FTR driver fuel shown in Table I was used as a basis, but several assumptions were made to simplify the calculations and to provide a broad, conservative basis for the nuclear safety evaluation. These assumptions are as follows:

- The fuel enrichment was assumed to be 20 vol% PuO_2-SS in all cases.
- The pins were assumed to be 0.20 in. diameter with no cladding.
- The PuO_2 was assumed to be at full theoretical density.
- The Pu^{240} content was assumed to be 5%.

TABLE I

FTR DRIVER FUEL DESCRIPTION

Fuel Pin Dimensions[a]	Subassembly
Diameter (unclad): 0.194 in.	No. of pins: 217, three of which are SS
Length (unclad): 36 in.	Arrangement of Pins: A hexagonal, close packed cluster; 8 rings plus 1 pin in center
Cladding: 0.008 in. steel	
Fuel Volume: 17.44 cm^3	Fuel Volume: 3.784 liters
Type 304 SS Composition	**PuO_2 Composition**
Iron: 74%	Pu^{239}: 93%
Chromium: 18%	Pu^{240}: 7%
Nickel: 8%	PuO_2 Density: 11.46 g/cm^3[b]
Density: 8.027 g/cm^3[b]	PuO_2 Content: 88.19%

Fuel per Subassembly

Vol% PuO_2	wt% PuO_2	wt PuO_2, kg	Total Weight, kg	g Cermet/ cm^3	g Pu/ cm^3	kg/Pu Subassembly
15	20.1	6.505	32.3	8.54	1.52	5.73
20	26.5	8.673	33.0	8.71	2.02	7.64

(a) Since completing this study, fuel pin dimensions have been changed to 0.210 in. diameter by 33.46 in. long. This change does not significantly change the conclusions of this report.

(b) Value used in computing fuel density.

Critical Parameters for FTR Fuel

The maximum material buckling for solid unmoderated FTR fuel is 14,700 x 10^{-6} cm^{-2}. The maximum material buckling for well moderated FTR pins in light water is 25,450 x 10^{-6} cm^{-2} (water-to-fuel volume ratio of 6.5). Extrapolation distances for FTR fuel reflected by water range from 7.3 cm (unmoderated fuel) down to 5.4 cm; for unmoderated fuel reflected by iron, the extrapolation distance is about 8.0 cm. This is shown in Table II and Figures 1 and 2.

TABLE II

CALCULATED CRITICAL PARAMETERS FOR 0.20 in. DIAMETER

20 vol% PuO_2-SS FUEL PINS IN LIGHT WATER

$\frac{Vol_{water}}{Vol_{fuel}}$	Center-to-Center Spacing Between Rods, cm	Buckling, 10^{-6} cm^{-2}	Extrapolation Distance for Full Water Reflection, cm			Minimum Critical Values		
			Sphere	Cylinder	Slab	Plutonium Mass, kg	Cylinder Diameter, in.	Slab Thickness, in.
0.5	0.593	17,790	6.45	6.60	6.87	28.21	8.99	3.86
1.0	0.684	19,583	6.41	6.54	6.80	17.47	8.38	3.49
4.0	1.082	24,626	6.09	6.20	6.34	4.58	7.19	2.89
6.0	1.280	25,400	5.96	6.05	6.16	3.14	7.12	2.90
9.0	1.530	25,252	5.82	5.89	6.99	2.30	7.28	3.06
13.0	1.810	24,046	5.68	5.75	5.83	1.87	7.69	3.39
17.0	2.052	22,360	5.58	5.65	5.73	1.73	7.21	3.76
19.0	2.164	21,450	----	5.61	5.69	1.70	8.51	3.97
21.0	2.269	20,523	5.51	5.58	5.65	1.70	8.83	4.19
23.0	2.380	19,600	5.48	----	----	1.72	----	----

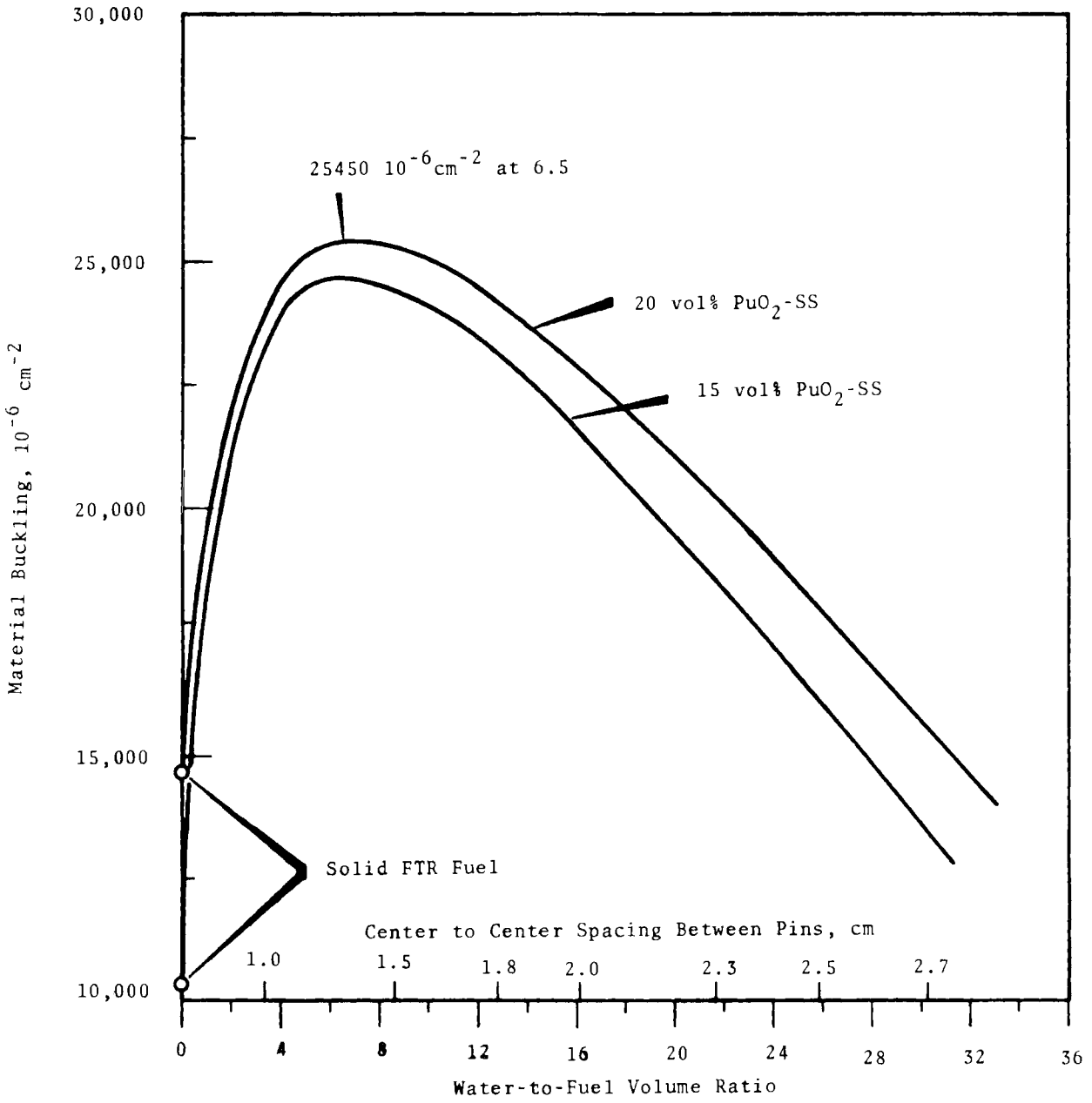

FIGURE 1

Material Buckling as a Function
of the Water-to-Fuel Volume Ratio
(0.20 in. diam pins)

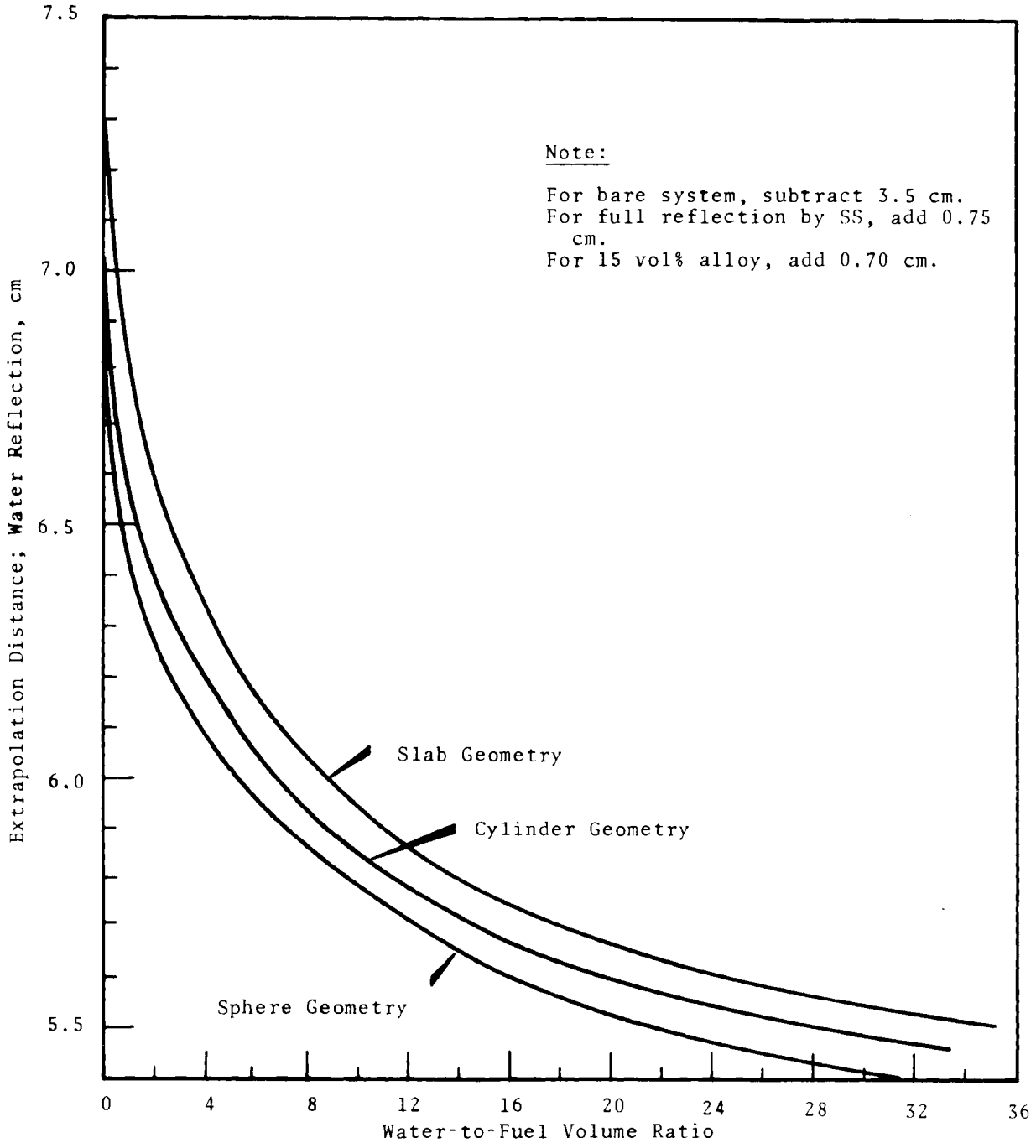

FIGURE 2

Extrapolation Distances for Full Water Reflection as a Function of the Water-to-Fuel Volume Ratio (0.2 in. diam 20 vol% PuO_2-SS pins)

Unmoderated FTR fuel in spherical geometry (i.e., solid cermet in the shape of a sphere) with no neutron reflection has a minimum critical mass of 119.8 kg plutonium (15.7 subassemblies); with full water reflection or equivalent, the minimum critical mass is 58.5 kg plutonium (7.6 subassemblies);[3] reflected by several inches of iron, the critical mass is reduced to 51.5 kg plutonium (6.7 subassemblies). Unmoderated FTR fuel in solid cylindrical geometry 36 in. long (rather than spherical) has a minimum critical mass of about 90 kg plutonium (11.8 subassemblies); unmoderated fuel pins 36 in. long bundled tightly together have a minimum critical mass of about 103 kg plutonium (13.5 subassemblies).

Moderated FTR fuel pins, 36 in. long, in light water in cylindrical geometry have a minimum critical mass of 3.11 kg plutonium (0.41 subassemblies) at a water-to-volume ratio of 21. In spherical geometry (rather than a 36 in. long cylinder) the minimum critical mass is reduced to 1.70 kg plutonium (0.22 subassemblies). Tightly packed pins in light water have a minimum critical mass of 47.5 kg plutonium (6.2 subassemblies) in a 36 in. long cylindrical geometry; and 28.2 kg plutonium (3.7 subassemblies) in spherical geometry (Table III and Figure 3).

For moderated FTR pins loosely arranged in light water, the minimum critical volume is 10.8 liter; the minimum critical cylinder diameter (infinite length) is 7.1 in.; and the minimum critical slab thickness (other dimensions infinite) is 2.88 in. For closely packed (water-to-fuel volume ratio of less than 0.5) FTR fuel pins in light water, the critical values are 20.9 liters, 10.1 in., and 4.47 in., respectively (Table III and Figures 4 through 6).

A summary of critical parameters for FTR fuel is presented in Table III.

TABLE III

SUMMARY OF MINIMUM CRITICAL PARAMETERS

FOR 20 vol% PuO_2-SS FTR FUEL

	Solid Unmoderated Cermet	36 in. Long Pins			Any Length Pins	
		Close Packed in Air	Close Packed in Water	Optimum Moderation	Close Packed in Water	Optimum Moderation
Maximum Buckling, 10^{-6} cm^{-2}	14,700	----	----	----	17,800	25,400
Minimum Critical Mass, kg/Plutonium	58.5[a]	130	47.5	3.11	28.2	1.70
No. of Subassemblies[b]	7.7	17.0	6.2	0.41	3.7	0.22
No. of Fuel Pins[c]	1662	3693	1349	88	801	48
Minimum Critical Volume, liters	29.0	----	----	----	20.9	10.8
Minimum Critical Slab Thickness, in.	4.47	----	----	----	3.85	2.88
Minimum Critical Cylinder Diameter, in.	10.1	----	----	----	9.0	7.1

(a) Full reflection by stainless steel reduces minimum critical mass to about 51 kg.

(b) Subassembly contains 7.683 kg plutonium.

(c) Fuel pin contains 35.2 g plutonium.

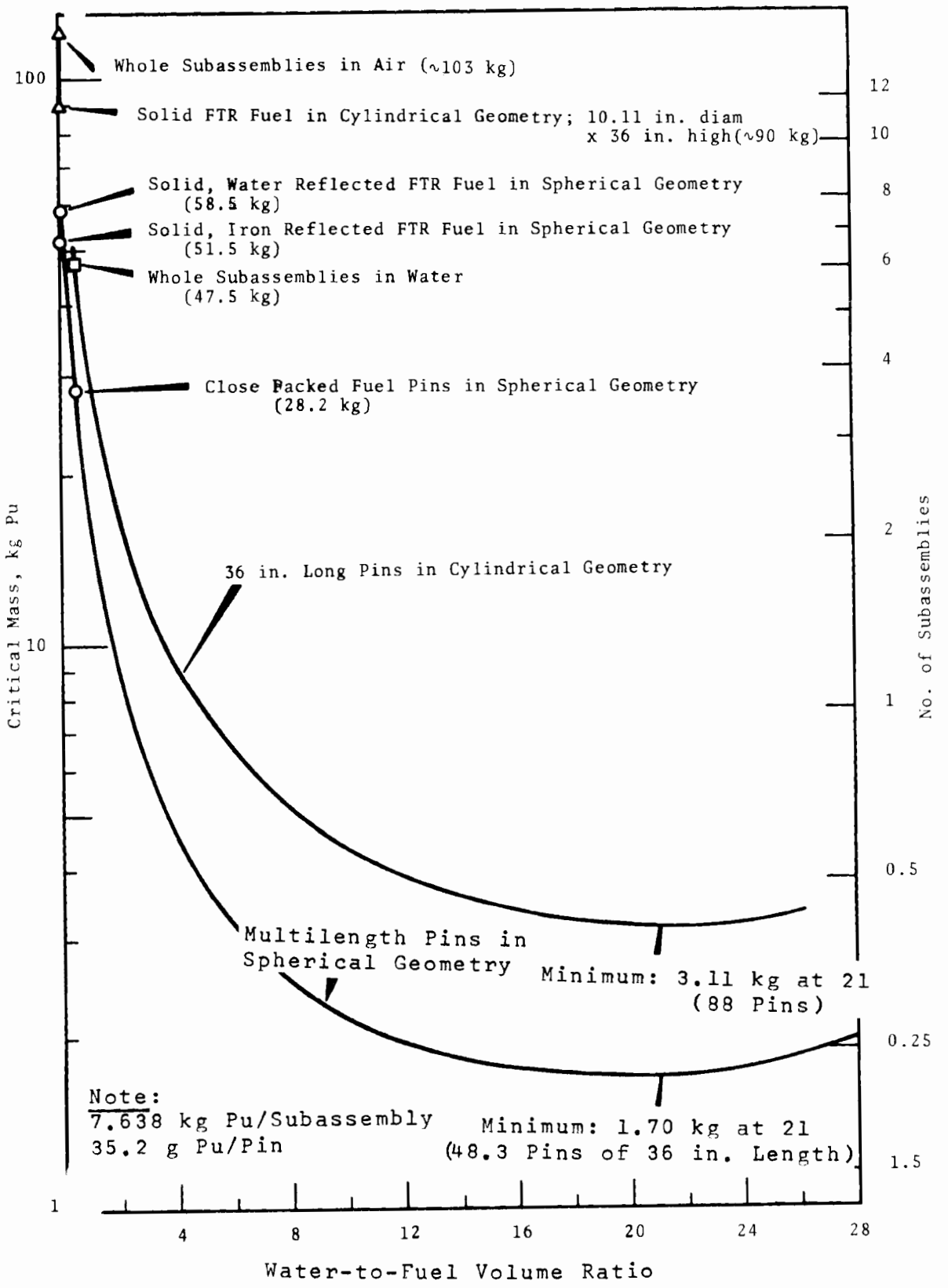

FIGURE 3

Critical Mass as a Function of the Water-to-Fuel Volume Ratio (0.2 in. diam 20 vol% PuO_2-SS pins; water reflected)

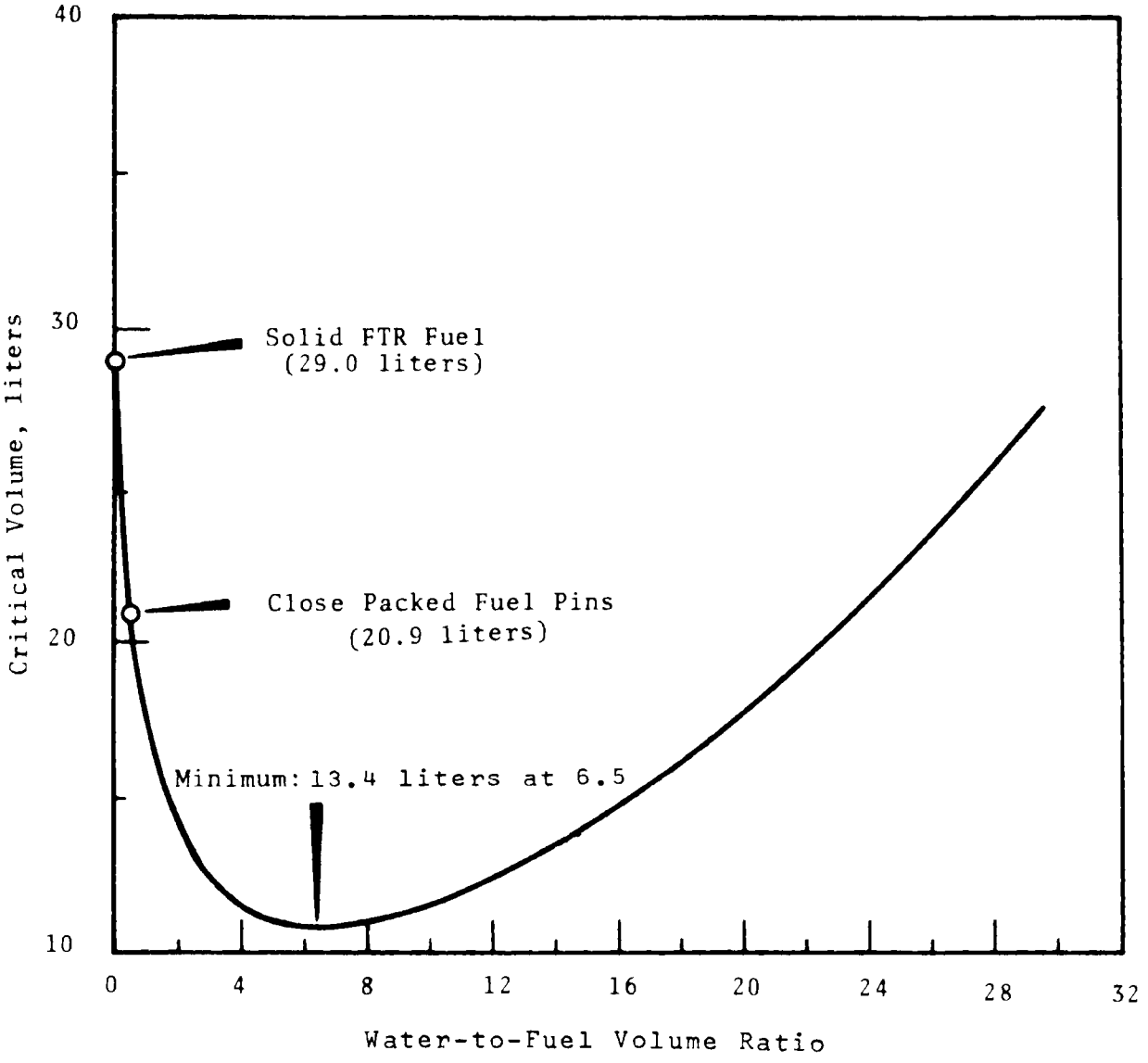

FIGURE 4

Critical Volume as a Function
of the Water-to-Fuel Volume Ratio
(0.2 in. diam 20 vol% PuO_2-SS pins;
spherical geometry; water reflected)

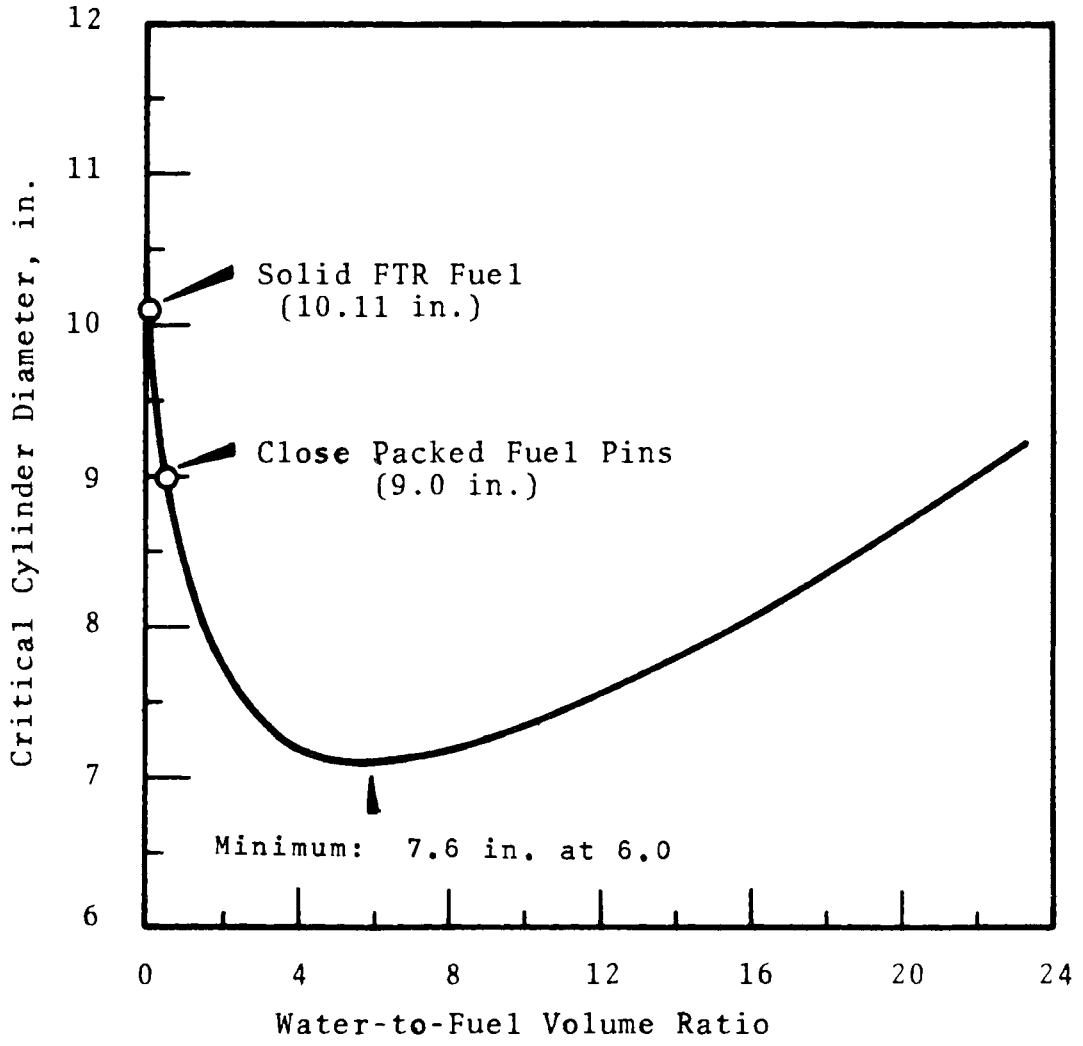

FIGURE 5

Critical Cylinder Diameter as a Function of the Water-to-Fuel Volume Ratio (0.2 in. diam 15 vol% PuO_2-SS pins; water reflected)

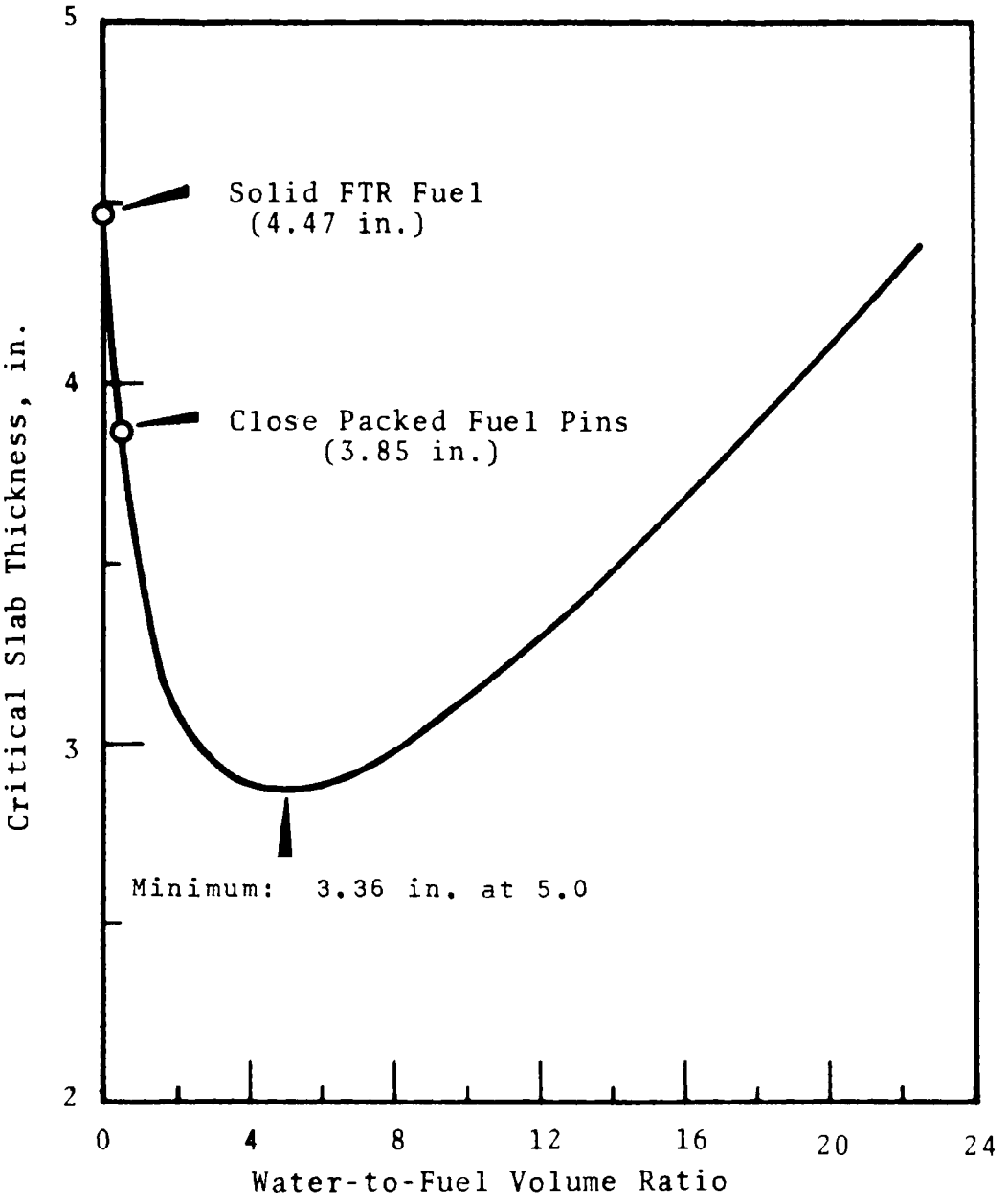

FIGURE 6

Critical Slab Thickness as a Function of the Water-to-Fuel Volume Ratio (0.2 in. diam 20 vol% PuO_2-SS pins; water reflected)

Criticality Safety of FTR Fuel Configurations

Fuel Subassemblies in Air

There is no possible way for one dry subassembly to reach criticality even in an accidental meltdown. Estimates of the number of dry subassemblies required for criticality under various conditions are as follows:

	Subassemblies Required for Criticality
Whole, Dry Subassemblies 36 in. long, side by side (water reflected)	~17
Meltdown into Cylindrical Geometry 36 in. long (water reflected)	11.8
Meltdown into Spherical Geometry (water reflected)	7.7
Meltdown into Spherical Geometry (steel reflected)	6.7

In any configuration, 5 dry integral subassemblies would be quite safe stored together but because of the marked effect of water on criticality and the credibility of flooding most storage arrays, the permitted batch limit is two subassemblies, spaced at least 3 ft from other fuel. A single layer of dry subassemblies may be stored horizontally in a row, side by side, or vertically in a single row side by side; but if dryness cannot be assured, the subassemblies would have to be spaced at least 12 in. apart, edge to edge in all directions. In practice the number of subassemblies permitted in an array will depend on spacing and credibility of flooding.

Fuel Subassemblies in Water

Even though it is not possible for one dry subassembly with 214 pins to become critical, regardless of pin geometry, as few as 48 pins can be critical if water moderation is present and the pins are in spherical geometry. Moderation can reduce the critical mass of the dry subassembly by a factor of 35.

For whole, closely packed subassemblies in water, at least six are required for criticality. Because of the water between subassemblies,

however, storage in water is limited to single subassemblies spaced at least 12 in. apart, edge to edge. This spacing is a minimum requirement and must be positively assured. The accidental dropping of one assembly, which crosses others in the array, will not cause criticality, provided that none of the subassemblies are broken and the 12 in. spacing between the other subassemblies is maintained. Subassemblies under water may not be stored side by side in rows.

Loose 36 in. Long Fuel Pins in Air

Fuel pins outside of dry glove boxes will be limited to lots of 10 pins. If safe geometry can be assured, however, a higher number of pins would be permissible. All other operations will be limited to 230 g plutonium, or covered by a special nuclear safety specification.

Loose 36 in. Long Fuel Pins in Water

For fuel pins that are loose, but whole, at least 88 pins are required for criticality. If geometry cannot be maintained, the number of pins handled together at one time must not exceed 30, with each batch spaced at least 12 in. apart edge to edge. An unlimited number of loose pins in water may be safely handled in cylindrical geometry not exceeding 5.5 in. ID, in slab geometry not exceeding 2.2 in. thick.

Loose Multilength Fuel Pins in Water

If the fuel pins are broken and of variable length, the minimum critical mass is 1.70 kg plutonium (equivalent to 48 pins 36 in. long). In this case, batches of broken pins in unconfined geometry should be limited to batches of 0.56 kg plutonium spaced at least 12 in. apart from other fuel. The safe cylinder diameter and slab thickness for broken pins is the same as for whole pins; 5.5 in. and 2.2 in., respectively.

Chemical Processing of FTR Subassemblies and Pins

When the PuO_2-SS cermet is dissolved in acid, it is expected that the PuO_2 will be separate from the steel. Criticality safety must therefore be based on the PuO_2-water system, with no allowance for neutron

absorption in the iron. Safe cylinder diameters and slab thicknesses for PuO_2 in water as a function of plutonium density are given in Table IV. Accumulations of over 230 g plutonium in uncontrolled geometry in any part of the reprocessing equipment must be avoided. Higher geometry and mass limits are possible by using fixed or soluble poisons such as Pyrex raschig rings, boron steel plates, gadolinium steel plates, or boron in solution.

TABLE IV

CRITICAL AND SAFE CYLINDER DIAMETERS AND SLAB THICKNESSES FOR PuO_2 IN WATER AS A FUNCTION OF PLUTONIUM DENSITY
(Full water reflection–no Pu^{240})(a)

Plutonium Density, g/cm^3	Infinitely Long Cylinder		Infinitely Wide and High Slab	
	Critical Diameter, in.	Safe Diameter, in.	Critical Thickness, in.	Safe Thickness, in.
1.0	6.05	5.14	2.05	1.74
1.6	5.75	4.89	1.88	1.60
2.5	5.26	4.47	1.59	1.35
4.0	4.97	4.22	1.43	1.22
5.0	4.69	3.99	1.29	1.10
6.0	4.48	3.81	1.19	1.01
8.0	4.09	3.48	1.01	0.86
10.0	3.81	3.24	0.86	0.73

(a) 7% Pu^{240} will increase the values listed by 10–20%, depending on plutonium density.

REFERENCES

1. L. L. Carter, C. R. Richey, C. E. Hughey. GAMTEC II: A Code for Generating Consistent Multigroup Constants Utilized in Diffusion and Transport Theory Calculations, BNWL-35. March, 1965.
2. J. R. Lilley. Computer Code HFN-Multigroup, Multiregion Neutron Diffusion Theory in One Space Dimension, HW-71545 (General Electric Company, Richland, Washington). November 17, 1961.
3. L. L. Carter. Personal communication. Battelle-Northwest, Richland Washington. June 28, 1965.

Measurements of Material Bucklings for 1.002, 1.25, and 1.95 wt% U^{235} Enriched Uranium Tube Lattices in Light Water

C. L. Brown and R. C. Lloyd

Introduction

Material bucklings and extrapolation distances have been measured for light water lattices of 1.002, 1.25, and 1.95 wt% U^{235} enriched uranium tubes, and 1.002 wt%/1.002 wt% and 1.25 wt%/0.95 wt% U^{235} enriched uranium tube-in-tube assemblies. The purpose of these measurements was to provide needed criticality safety data for the General Electric Company, N-Reactor Department, who are fabricating, storing, and trasporting tubular fuels; and to provide additional experimental data for correlation to theoretical methods.

Most of the criticality measurements that have been performed to date on heterogeneous systems of slightly enriched uranium in light water have been with solid rods; comparatively few experiments have been performed with tubular fuels. Prior to the present study, buckling measurements were available for only the following tube sizes and enrichments: 1.007, 1.25, 1.44, 1.466, and 1.6 wt% U^{235} enriched tubes measured at Hanford;[1-5] 0.95 wt% U^{235} enriched tubes measured at ORNL;[6] and 0.95 wt% enriched tubes and 0.95 wt% enriched tube-in-tube assemblies measured at Savannah River Laboratory.[7]

The uranium tubes measured at Hanford and ORNL in the past were all nearly of the same diameter (1.37 in. OD, 0.48 in. ID), so the experimental data did not show the effect of tube size on material buckling. The tubes measured at SRL were of a larger diameter (1.91 in. OD, 1.23 in. ID) and permitted the first comparison of the effect of tube size, and the measurements on the tube-in-tube assemblies were the first available for this type of fuel. However, the SRL measurements were at a relatively low enrichment.

In the present study, measurements on three larger diameter tubes and two tube-in-tube assemblies are reported. A drawing showing the tube diameters and enrichments that have now been measured to date, including the present study, is given in Figure 1.

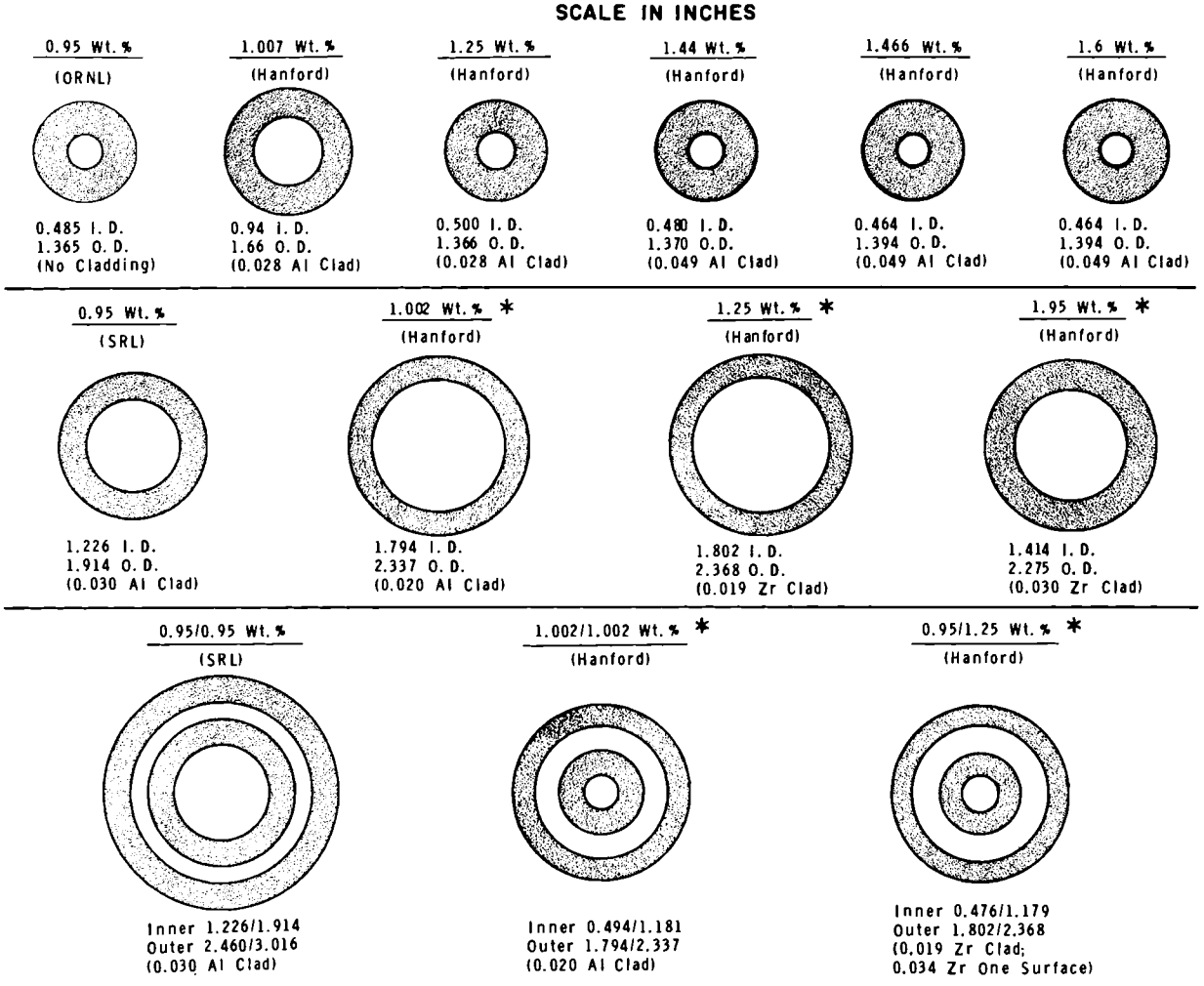

FIGURE 1

Comparison of Tube Diameters and U^{235} Enrichments for Which Material Bucklings Have Been Measured

Experimental Methods

Exponential Measurements

The standard exponential experimental method was used to obtain material bucklings and extrapolation distances for the 1.002 and 1.25 wt% U^{235} tubular fuels. For each fuel, vertical flux traverses were performed on two fuel column diameters at each of three lattice spacings: 2.8, 3.1, and 3.4 in. The 1.002 wt% fuel columns were 42 in. long and the 1.25 wt% columns were 52.4 in. long. The sides and bottom of each uranium column were fully reflected with water. The water height in the tank was adjusted to remain level with the top surface of the uranium tubes.

Critical Approach Measurements

Material bucklings for 1.95% enriched tubes were obtained using the approach-to-critical technique. The experiments were carried out in a 4 ft diameter by 6 ft high water tank in the thermal test reactor room of the 305-B Building. The lattice spacings and fuel arrangements were the same as used in the exponential experiments. The fuel columns were fully reflected on all sides by water. Neutron multiplication was observed on three BF_3 channels: one BF_3 counter was placed at the center of the lattice a few inches above the source; and the other two were placed in the reflector at the edge of the fuel loading.

Measurements on the 1.95 wt% tubes were performed at two uranium heights: 27.3 and 40.3 in. The 40.3 in. columns were comprised of a 27.3 and a 13.0 in. tube. It was originally believed that by measuring two fuel heights and equating bucklings, reliable extrapolation lengths could be obtained. This was not possible, however, because of perturbations caused by the end caps at the junction of the 27.3 and 13.0 in. tubes. Consequently, material bucklings were calculated based on the critical size of the 27.3 in. fuel columns and assuming extrapolation lengths from the previous 1.002 and 1.25 wt% measurements.

Results

The material bucklings and extrapolation distances obtained from the experimental measurements are given in Tables I and II.

TABLE I

RESULTS OF EXPONENTIAL MEASUREMENTS

Lattice Spacing, in.	$\frac{V_w}{V_u}$	No. Tubes	R_{eff}, cm	b, cm	λ, cm	B^2, M^{-2}
	Tubes - 1.002 wt% U^{235} (1.794 in. ID, 2.337 in. OD)					
2.40	1.60	37	19.47	13.54	8.51	19.31
		55	23.74	16.60		
2.80	2.64	37	22.71	15.81	7.34	24.34
		55	27.69	20.94		
3.10	3.51	37	25.15	15.91	7.70	14.11
		55	29.52	19.03		
3.40	4.47	37	27.58	14.40	7.2(a)	-0.42
	Tubes - 1.25 wt% U^{235} (1.802 in. ID, 2.368 in. OD)					
2.40	1.57	37	19.52	17.95	8.20	44.36
2.80	2.53	19	16.28	13.66		
		37	22.71	18.50	7.82	46.24
3.10	3.36	19	18.02	14.05		
		37	25.15	24.95	7.58	37.89
3.40	4.27	19	19.76	13.24		
		37	27.58	19.73	7.32	21.80
Assemblies - Inner Tube: 1.002 wt% U^{235} (0.494 in. ID, 1.181 in. OD) Outer Tube: 1.002 wt% U^{235} (1.794 in. ID, 2.337 in. OD)						
2.40	0.68	55	23.74	12.72	8.5(a)	-6.17
2.80	1.35	37	22.71	15.50	7.8	20.49
		55	27.69	19.84		
3.10	1.93	37	25.15	17.91	7.7	22.55
		55	29.52	22.78		
3.40	2.56	37	27.58	17.07	7.0(a)	14.04
Assemblies - Inner Tube: 0.95 wt% U^{235} (0.476 in. ID, 1.179 in. OD) Outer Tube: 1.25 wt% U^{235} (1.802 in. ID, 2.368 in. OD)						
2.40	0.66	37	19.52	13.00	8.40	15.04
2.80	1.30	19	16.28	12.30		
		37	22.71	18.50	7.92	32.44
3.10	1.86	19	18.02	13.74		
		37	25.15	24.50	7.13	38.84
3.40	2.47	19	19.76	13.62		
		37	27.58	21.83	6.83	27.85

(a) Estimated from plot of measured λ versus H_2O/U volume ratio.

TABLE II

RESULTS OF CRITICAL APPROACH MEASUREMENTS ON 1.95 wt% U^{235} TUBES

(1.414 in. ID, 2.275 in. OD)

Lattice Spacing, in.	$\frac{V_w}{V_u}$	Fuel Height, in.	Critical No. of Tubes[a]	Critical R_{eff}, cm	λ, cm[b]	B^2, M^{-2}
2.80	1.58	27.3	30.96	20.78	8.4	81.22[c]
		40.3	28.43	19.91		
3.10	2.19	27.3	26.48	21.27	7.9	81.59
		40.3	21.36	19.11		
3.40	2.87	27.3	27.88	23.94	7.6	71.94
		40.3	24.44	22.42		

(a) Estimated from least squares fit of inverse multiplication measurements.

(b) Extrapolation lengths were assumed to have values similar to those for 1.002 wt% and 1.25 wt% U^{235} enriched tubes.

(c) The bucklings computed from data on the 27.3 in. high cylinders; the cylinders of 40.3 in. height require correction for the effect of end caps.

It is interesting to note that for the 1.25 wt% fuel, even though the lattices were quite far from criticality, the inverse neutron multiplication curves were nearly linear; and gave critical numbers of tubes quite close to the numbers calculated from material buckling (see Figure 2). The critical number of tubes predicted by a least squares fit of the inverse multiplication curves for the 2.8 and 3.1 in. lattices were 62.3 and 64.4, compared to 62.0 and 67.9, respectively, calculated from measured bucklings. The results of the multiplication measurements with the 1.95 wt% U^{235} enriched tubes of 27.3 in. height are plotted in Figure 3. The bucklings and extrapolation distances obtained are plotted in Figures 4, 5, and 6. Note in Figure 6 that the measured extrapolation distances resulted in two distinct curves: one for tubes and one for tube-in-tube assemblies.

Based on the experimental data, critical masses, volume, cyclinder diameters, slab thicknesses, and masses per unit area were calculated for each of the uranium tubes measured. These parameters are given in Table III.

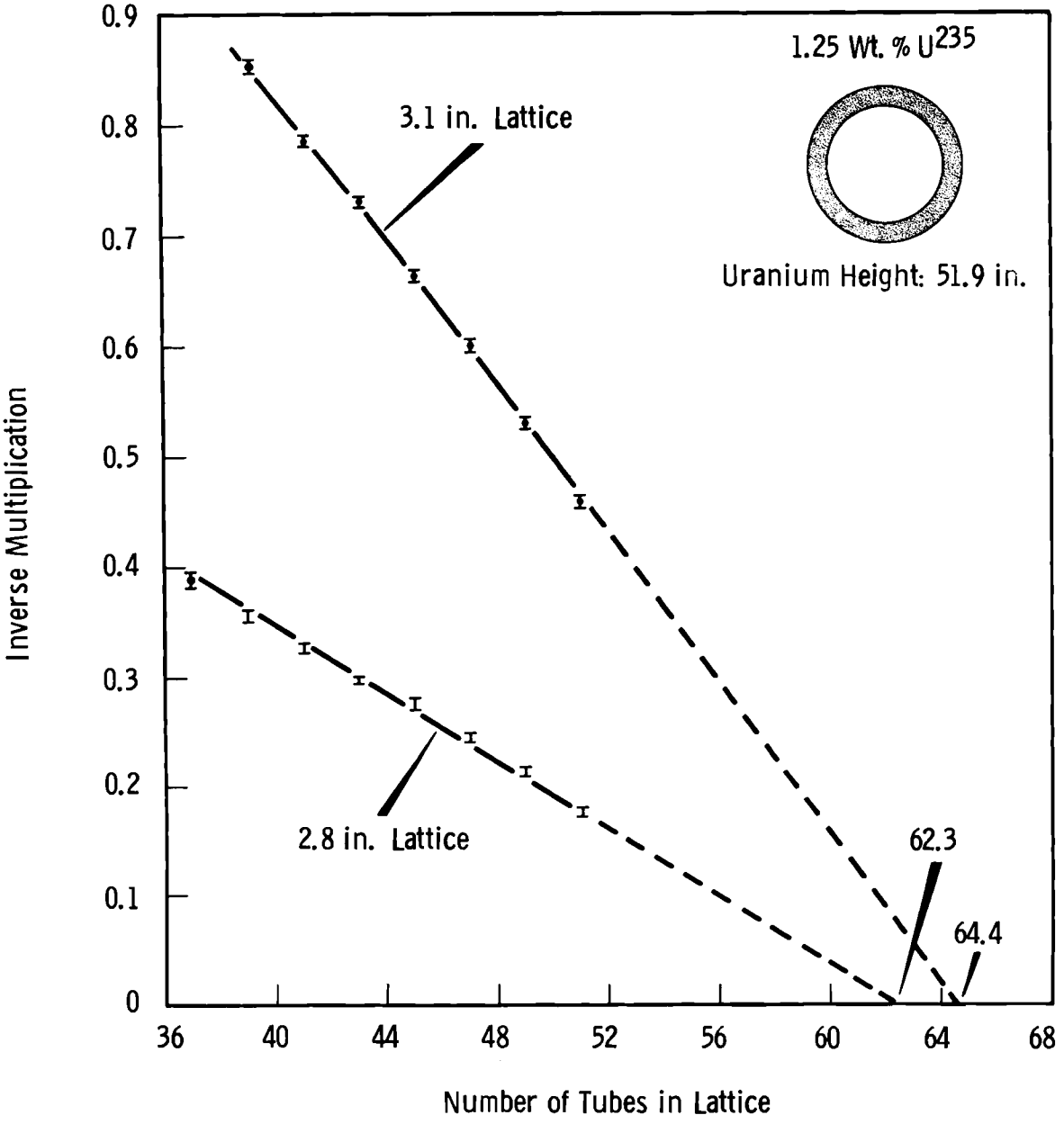

FIGURE 2

Multiplication Measurements Obtained
During 1.25 wt% U^{235} Enriched Fuel Load
of 2.8 and 3.1 in. Lattices

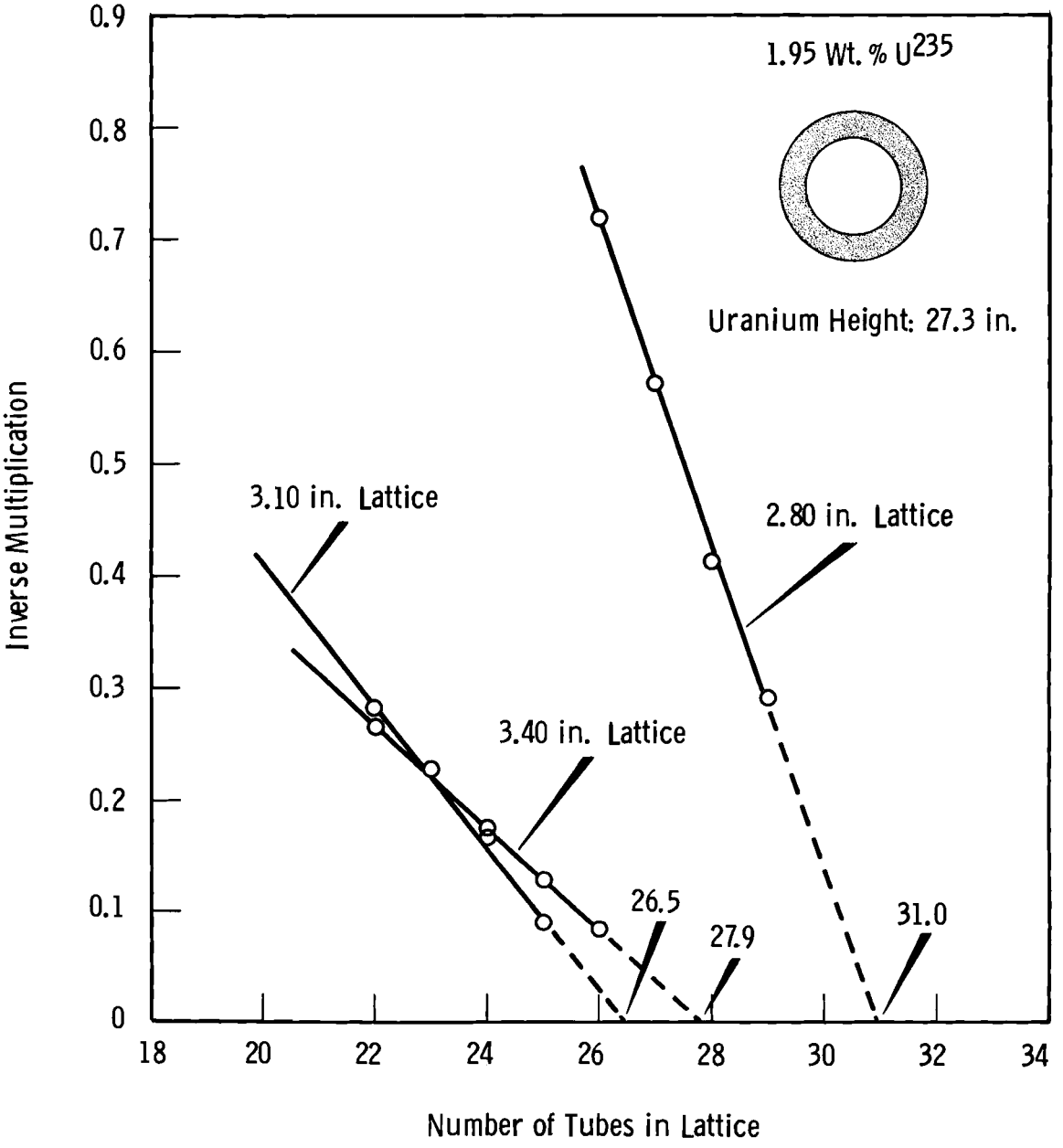

FIGURE 3

Results of Critical Approach Measurements on 1.95 wt% U^{235} Tubes at 27.3 in. Height

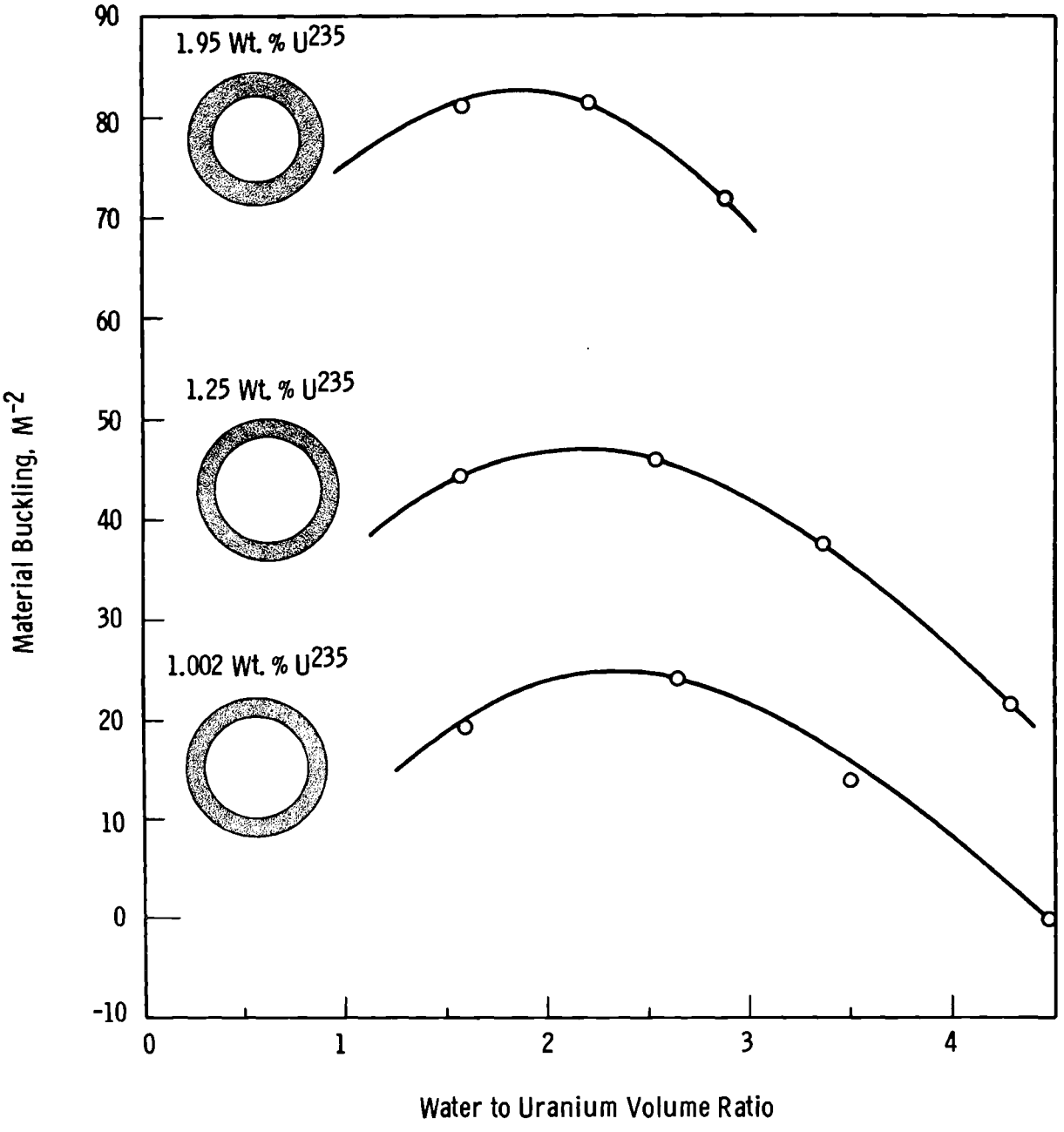

FIGURE 4

Measured Bucklings for Tubes

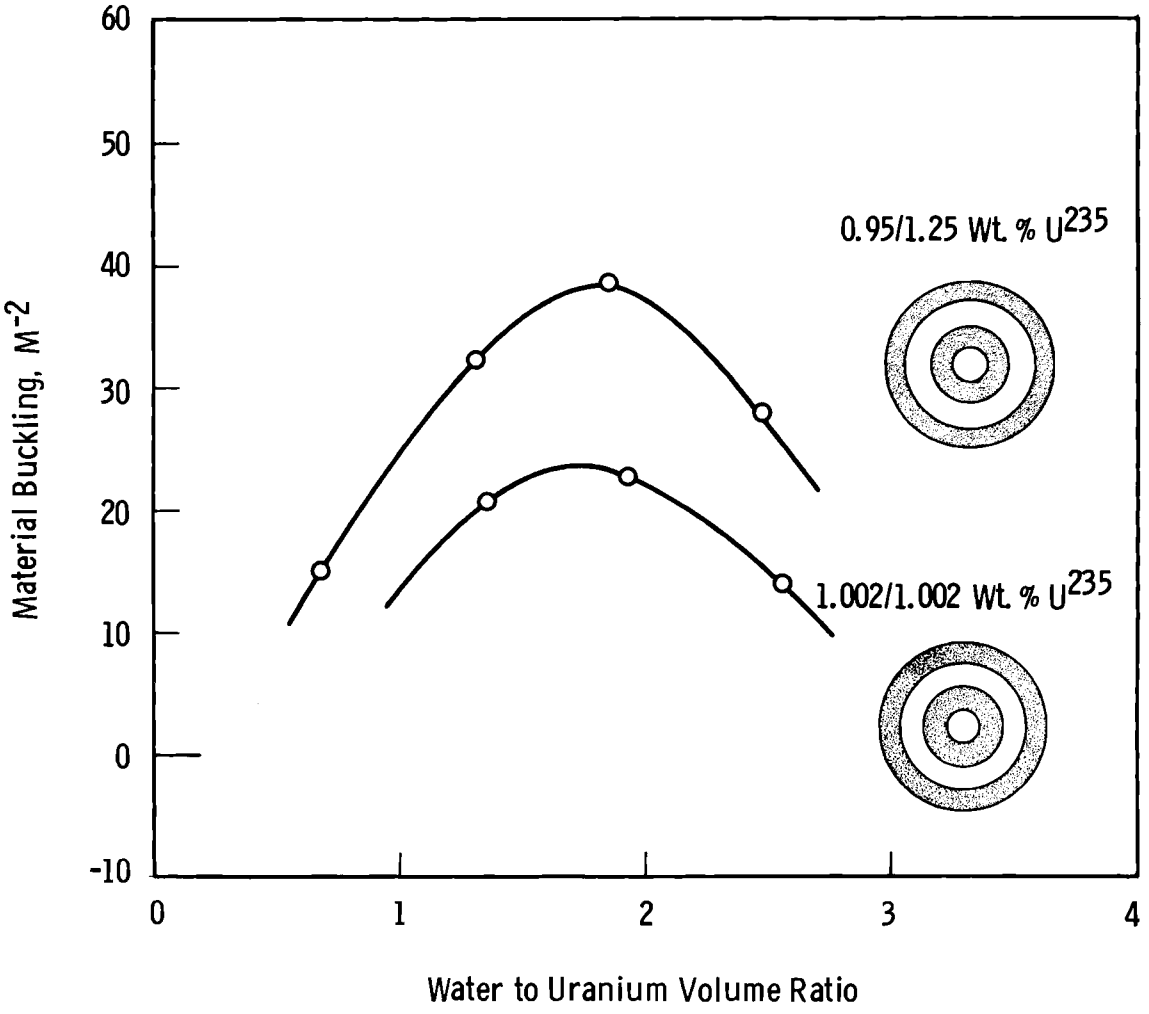

FIGURE 5

Measured Bucklings
for Tube-in-Tube Assemblies

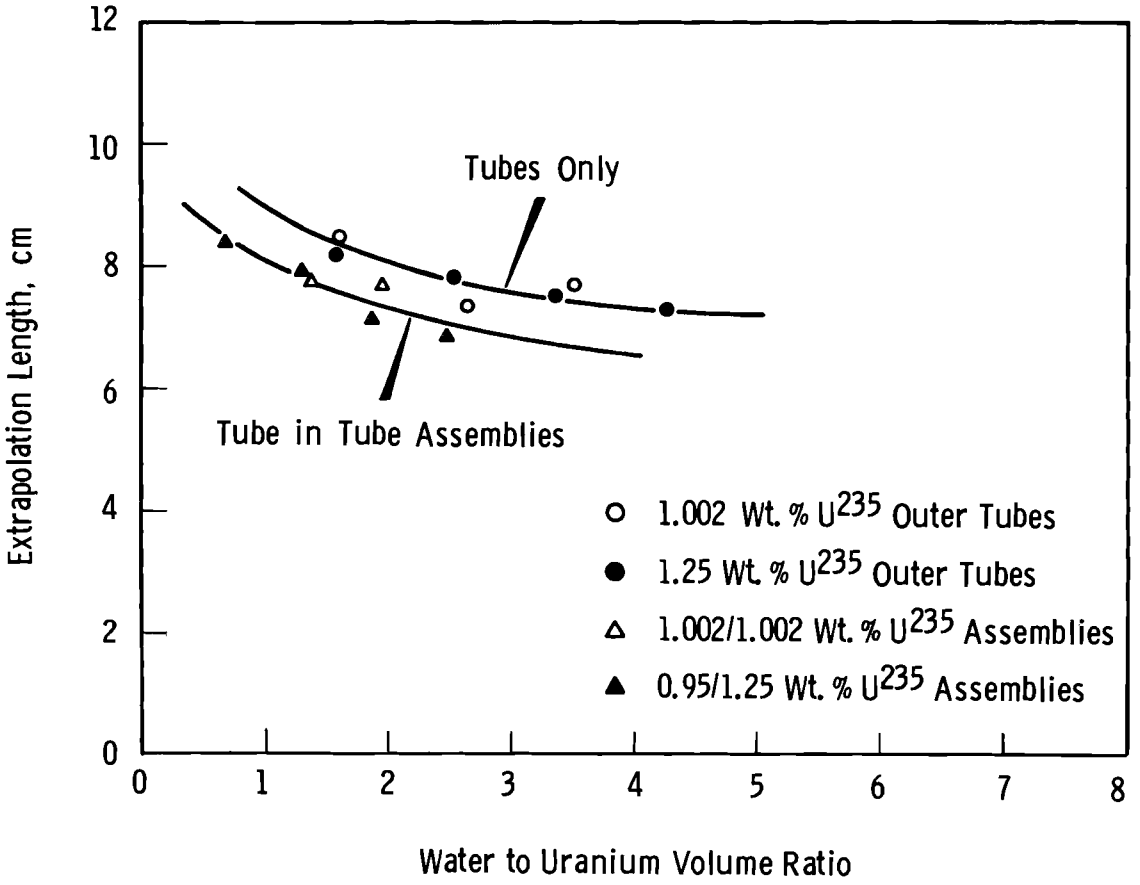

FIGURE 6

Measured Extrapolation Lengths

TABLE III

CRITICAL PARAMETERS FOR THE TUBES AND ASSEMBLIES USED IN THE MEASUREMENTS CALCULATED FROM EXPERIMENTAL DATA

$\frac{V_w}{V_u}$	Minimum Critical Values: Mass, lb. U	Volume, gal	Slab Thickness, in.	Cylinder Diameter, in	Mass per Unit Area, lb U/ft^2
Tubes - 1.002 wt% U^{235}					
1.60	15,410	276.5	21.5	36.4	765.2
2.64	8,110	197.9	19.3	32.6	499.4
3.51	16,180	484.5	26.8	44.4	565.6
Tubes - 1.25 wt% U^{235}					
1.57	3,799	65.5	12.1	22.0	438.1
2.53	2,681	62.6	12.0	21.7	321.4
3.35	3,177	90.8	14.1	24.8	308.1
4.27	6,946	238.6	34.8	34.8	376.0
Tubes - 1.95 wt% U^{235}					
1.58	1,183	20.5	7.11	14.4	255.9
2.19	1,012	21.5	7.47	14.7	219.5
2.87	1,106	28.2	8.60	16.3	210.0
Assemblies - 1.002/1.002 wt% U^{235}					
1.35	16,287	258.7	21.2	35.7	831.4
1.93	11,296	221.1	20.0	33.8	636.6
2.56	21,302	502.1	27.5	45.0	727.2
Assemblies - 0.95/1.25 wt% U^{235}					
0.66	36,921	423.6	25.3	42.2	1,370.3
1.30	7,512	116.7	15.5	27.0	620.0
1.86	4,702	89.7	14.2	24.8	463.9
2.47	7,058	162.0	18.1	30.5	489.5

Attempts to accurately calculate material bucklings for slightly enriched uranium tubes using multigroup diffusion theory have to date been only moderately successful.[8] Calculated bucklings are larger than the exponential bucklings by approximately 10 m^{-2}. This difference corresponds to an error of about 3% in k_∞. To improve the theoretical model, further consideration is being given to the method used for calculating the

effective surface area of a tube, which is necessary for estimating resonance escape; and to the method of calculating thermal utilization. The application of the Adler-Nordheim method for calculating resonance integrals, and the THERMOS code for improving the calculation of thermal utilization, are currently under evaluation. The experimental results obtained in the present study are expected to be of considerable value in verifying the calculational method.

REFERENCES

1. E. A. Block, and E. D. Clayton. "Buckling Measurements with Enriched Fuel Elements in Light Water," Nuclear Physics Research Quarterly Report, July, August, September, 1956, HW-47012, pp. 12-17 (General Electric Company, Richland, Washington). October, 1956.
2. R. C. Lloyd. "Exponential Measurements with 1.25 Percent Enriched Uranium," Nuclear Physics Research Quarterly Report, January, February, March, 1959, HW-60220, pp. 55-57 (General Electric Company, Richland, Washington). April, 1959.
3. E. Z. Block. "Enriched Uranium-Water Lattices," Nuclear Physics Research Quarterly Report, October, November, December, 1956, HW-44893, pp. 43-44 (General Electric Company, Richland, Washington). January, 1957.
4. E. Z. Block. "Enriched Uranium-Water Lattices," Nuclear Physics Research Quarterly Report, April, May, June, 1957, HW-51983, pp. 49-54 (General Electric Company, Richland, Washington). July, 1957.
5. R. C. Lloyd. "Nuclear Safety Specification for Enriched Uranium in the 1.25 - 2 Percent Range," Nuclear Physics Research Quarterly Report, January, February, March, 1958, HW-55879, pp. 9-12 (General Electric Company, Richland, Washington). April, 1958.
6. J. K. Fox and L. W. Gilley. "Critical Parameters of Slightly Enriched Annular Cylindrical Uranium Metal Slugs," Neutron Physics Division Annual Progress Report for Period Ending September 1, 1959, ORNL-2842 (Oak Ridge National Laboratory). November 16, 1959.
7. W. B. Rogers, Jr. Savannah River Laboratory, Personal Communication. May, 1963.
8. C. R. Richey, R. C. Lloyd, and E. D. Clayton. "Criticality of Slightly Enriched Uranium in Water Moderated Lattices," Nuclear Science and Engineering, vol. 21, p. 217. 1965.

Neutron Interaction Between Multiplying Media Separated by Various Materials

J. D. White and C. R. Richey

Introduction

The quantity of material necessary to effectively isolate a multiplying media is of primary concern to the design of shipping containers and formulation of storage regulations for fissionable materials. To date, however, there has been a lack of information on the isolating properties of several materials of interest. This report gives the results of a series of critical experiments in which the isolating properties of various materials were investigated. Those materials tested were placed at the interface between two arrays of multiplying media that comprised the core of a critical assembly. The critical length of the fuel core was then determined as a function of the test material thickness; the effective isolation thickness of a material was taken to be that thickness for which the fuel core critical length approached an asymptotic value. Comparative data were also obtained on the reflector savings associated with the various test materials, where the reflector savings is defined as the decrease in critical length due to the presence of the reflector.

Description of Experiments

The critical arrays were assembled with the remotely operated split-table device, the RSTM, located in a large glove box at the Battelle-Northwest Critical Mass Laboratory.[1] The experimental assemblies consisted of 2 in. PuO_2-polystyrene cubes alternated with 2 in. Plexiglas cubes to form an array resembling a three dimensional checkerboard. The resulting heterogeneous array had an average plutonium concentration of 0.56 g/cm^3 with an H/Pu atomic ratio of 35.6 (as compared to 1.12 g/cm^3 of Pu and H/Pu = 15 for the fuel compacts). Use of this checkerboard arrangement provided a more thermalized spectrum than was obtainable with an array consisting only of the PuO_2-polystyrene compacts. The fuel core had cross sectional dimensions of 30.632 x 30.886 cm and was divided lengthwise into two arrays. The length of one array was held constant at 5.16 cm, while the length of the second array was varied to achieve criticality.

Various test materials were inserted at the interface between the two sections of the core, with the critical length of the variable core determined as a function of the test material thickness; i.e., the effect of the fixed core on the critical length of the variable core was measured for several thicknesses of each test material. To determine this effect, the critical length of the variable array was first determined with the test material in place, but with the fixed core removed; then the critical length was remeasured with the fixed core in place on the opposite side of the interface from the variable core. The ratio, R, of the critical length of the variable core with the fixed core in place to the critical length of the variable core with the fixed core removed was taken as a measure of the effective isolation of the fixed core. When this ratio became unity the fixed core was said to be isolated from the variable core and the thickness of the test material between the two core sections was called the isolation thickness of the material. For purposes of this report, however, the thickness of test material required for the ratio, R, to equal 0.999 was defined as the effective isolation thickness. Figure 1 shows the relative positions of the fixed and variable cores and the test material for a typical measurement.

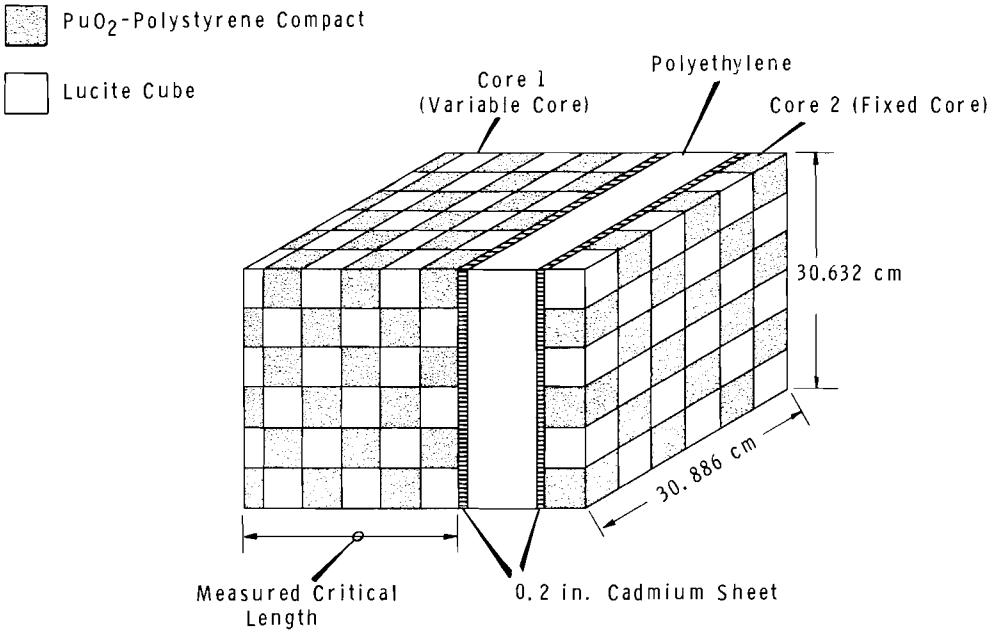

FIGURE 1

Typical Array Used in Isolator Measurements

Experimental Results

The experiments were performed over an interval of several months and changes necessarily occurred to the environment of the experimental facility as well as to the assembly itself. These changes caused corresponding variations in the experimental data. To eliminate errors of this nature, the experiments were normalized to a basic array, consisting of the bare checker-board assembly for which criticality was determined periodically throughout the series of experiments. Since the measurements were performed relative to the basic array, effects from the rubberized plastic coating on the fuel blocks, and neutron reflection from nearby object, should cancel.

Each 2 in. cube of PuO_2-polystyrene generated about 0.3 W of thermal heat from alpha emission,[2] hence the temperature of the assembly varied considerably during the course of experiments. Thermocouples recorded the temperature at several locations throughout the assembly. To correct for the temperature variations, the source-neutron multiplication was measured as a function of temperature in the slightly subcritical bare array. Observed variations in the source-neutron multiplication with temperature were applied directly to the inverse multiplication data defining criticality of each experimental array; all data were corrected to a median temperature of 50 °C.

In Figure 2 through 9 are summarized the experimental results for each material tested. The upper curve in each figure shows the decrease in the critical core length with one end of the assembly reflected with various thicknesses of test material. This decrease in the critical length defines the reflector savings for each material as a function of thickness; the thickness at which each material is an effective infinite reflector is defined as the respective curves approach an asymptotic value. The lower curve in each figure illustrates the isolation effect due to varying thicknesses of the materials placed at the interface of Core 1 and Core 2 (Figure 1). It is interesting to note that when thin pieces of polyethylene and compressed wood are inserted at the interface, the critical length of Core 1 decreases to a minimum at a thickness of about 2 cm. This minimum occurs primarily because neutron moderation in the isolators is the dominant effect, but as

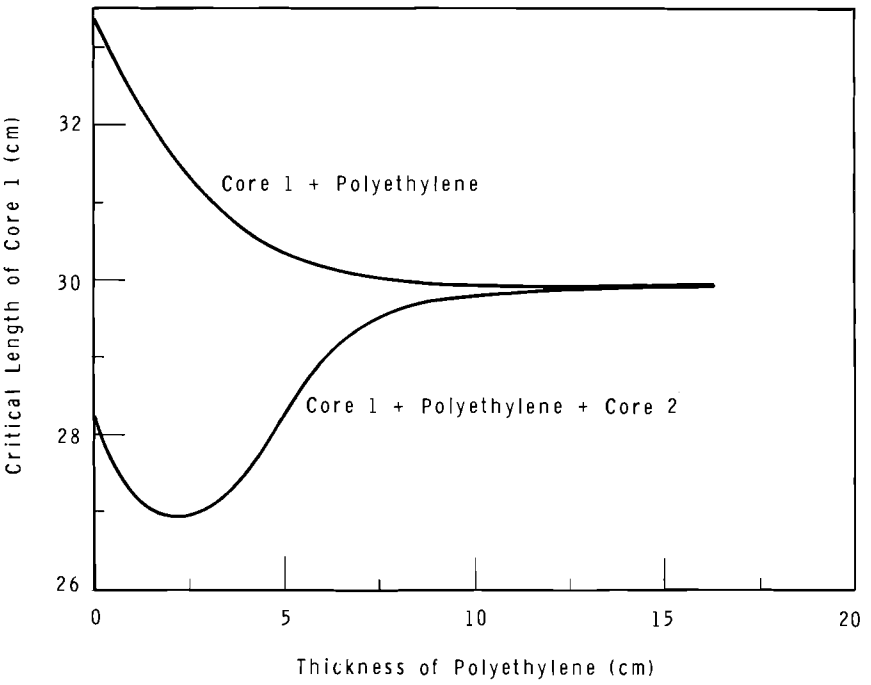

FIGURE 2

Polyethylene as Isolator

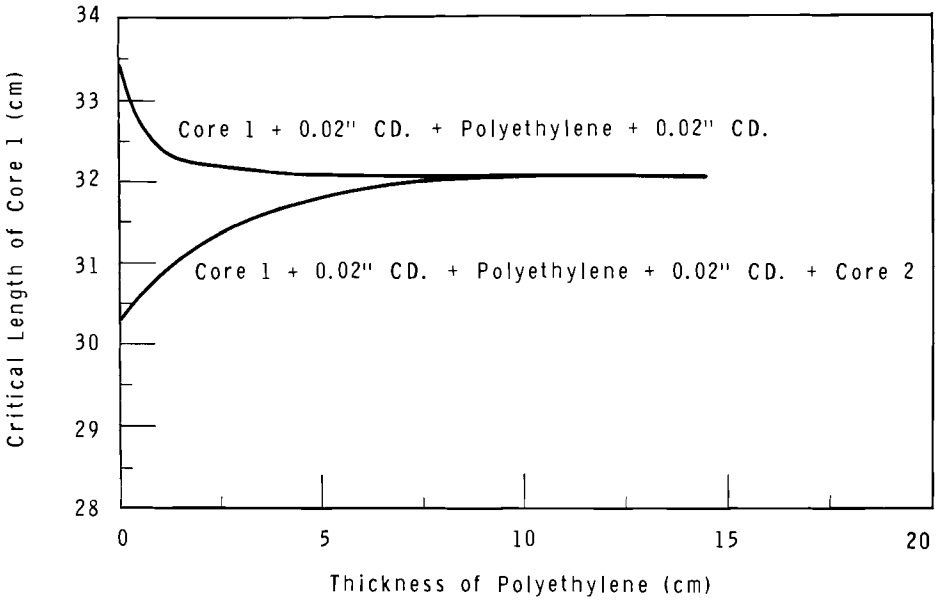

FIGURE 3

Polyethylene and Two Sheets of Cadmium as Isolator

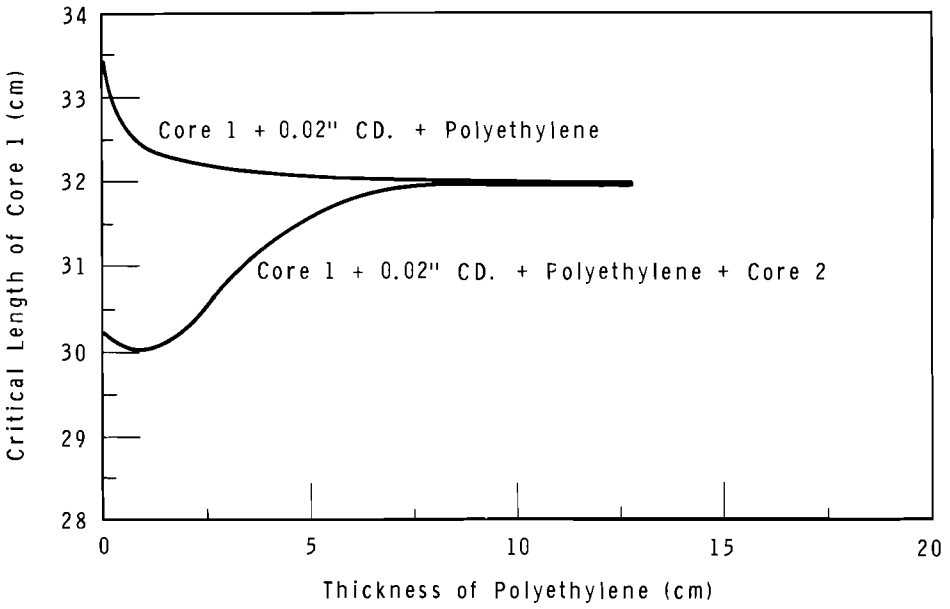

FIGURE 4

Polyethylene and One Sheet of Cadmium as Isolator

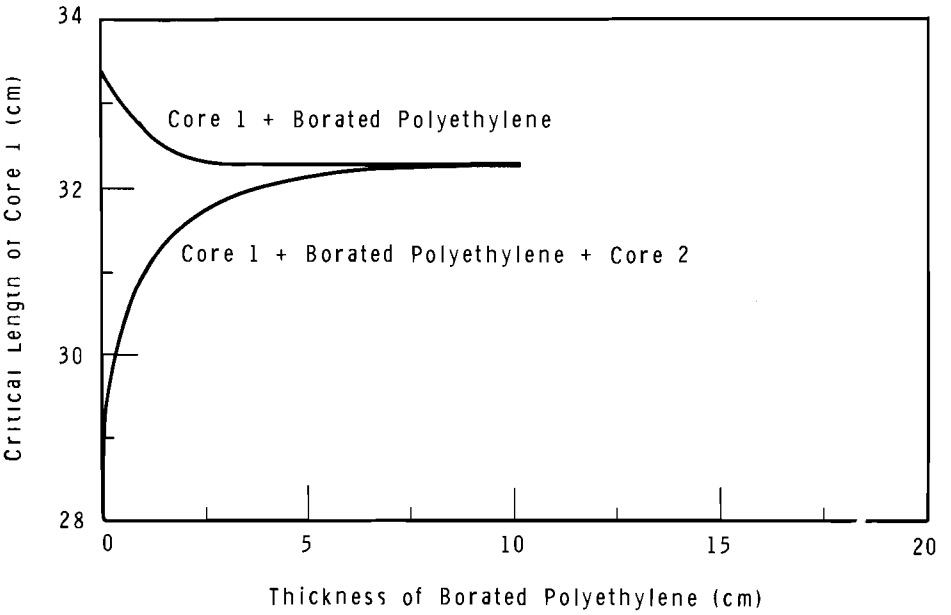

FIGURE 5

Borated Polyethylene as Isolator

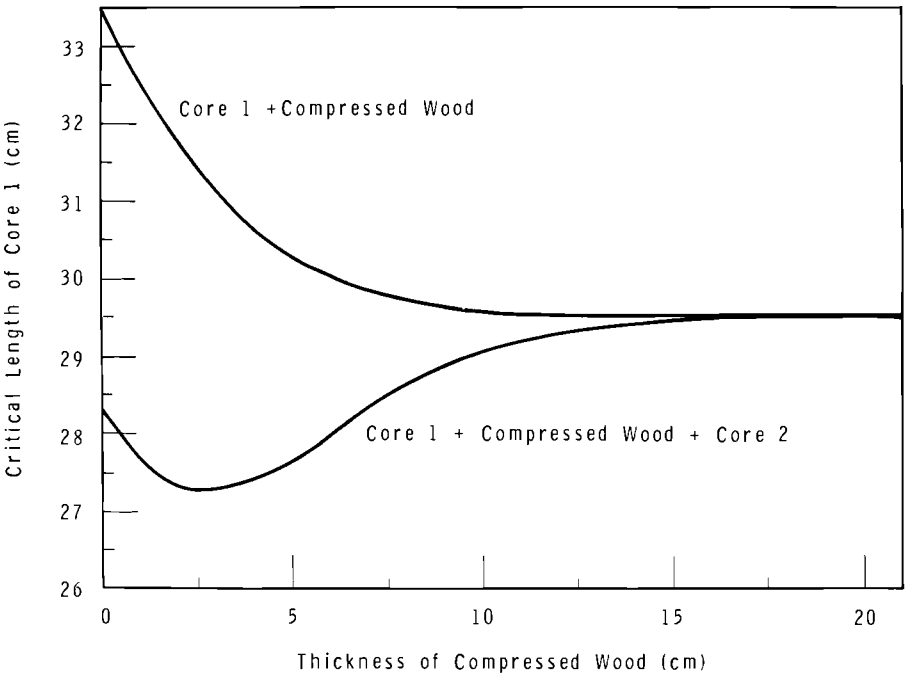

FIGURE 6
Compressed Wood as Isolator

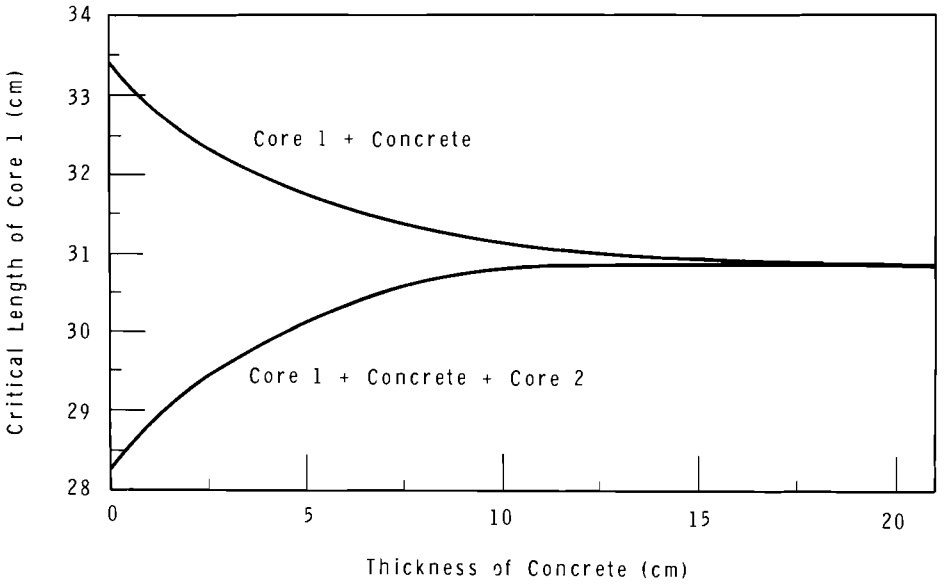

FIGURE 7
Concrete as Isolator

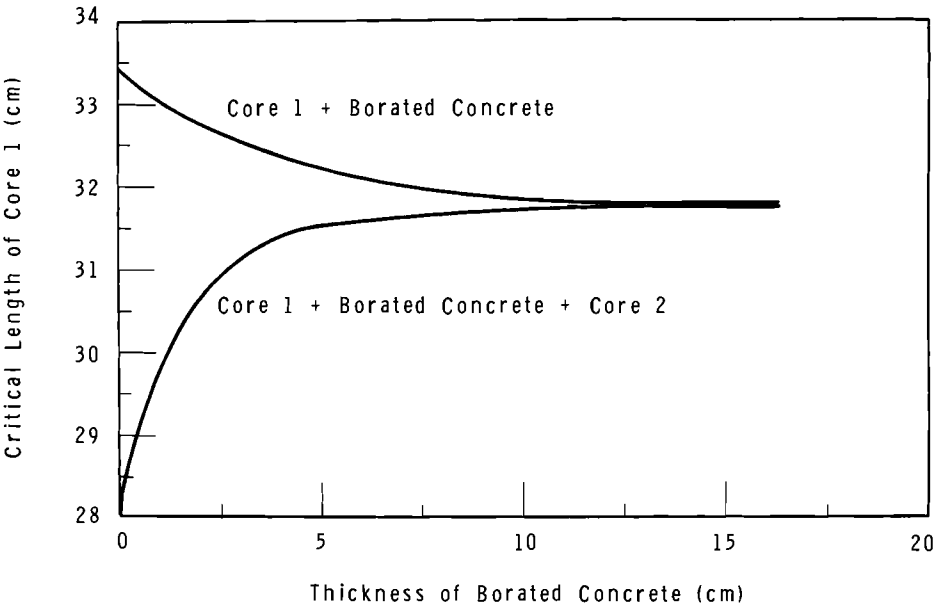

FIGURE 8

Borated Concrete as Isolator

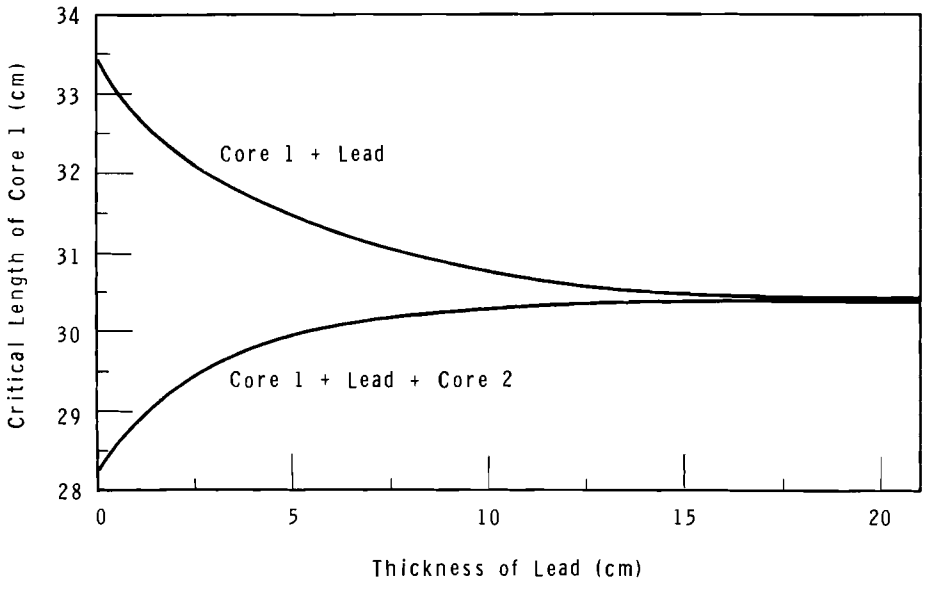

FIGURE 9

Lead as Isolator

the isolator thickness increases, reduction of neutron interaction between fuel cores becomes dominant. As seen in Figure 3, the minimum is reduced by inserting a 0.02 in. cadmium sheet at the Core 1-polyethylene interface. Also, the minimum is eliminated by either inserting another cadmium sheet at the Core 2-polyethylene interface, or on replacing the polyethylene with borated polyethylene. For concrete and lead, which are rather inefficient moderators, the isolation curves show an asymptotic increase with material thickness, Figures 7 and 9. Table I lists the densities of the various isolator materials studied.

TABLE I

ISOLATOR DENSITIES

Isolator Material	Density, g/cm^3
Polyehtylene	0.917
Borated Polyethylene (10 wt% Boron)	0.964
Compressed Wood	1.341
Concrete	2.33
Borated Concrete (2.2 wt% Boron)	2.33
Lead	11.34
Cadmium	8.37

In Table II are recorded the effective isolation thicknesses and their respective reflector savings for the test materials. Evident from these results is that a considerable reduction in the isolation thickness may be obtained by the addition of neutron absorbers. It is also evident that by adding neutron absorbers to the isolating material, the critical mass of the isolated unit is increased, permitting larger quantities of fissile material to be stored in the array.

Figure 10 shows the effect of neutron interaction between Core 1 and Core 2 as a function of void thickness. With the various test materials separating Core 1 and Core 2, the effects due to interaction alone are determined by substracting out the neutron reflection contributions to the data. The interaction effects are illustrated in Figures 11 and 12 where the quantity

TABLE II

SUMMARY OF EXPERIMENTAL RESULTS

Material	Reflector Savings, cm	Effective Isolation Thickness, cm
Polyethylene	3.52 ± 0.05	17.5 ± 0.5
Polyethylene*	1.50 ± 0.05	10.8 ± 0.2
Polyethylene**	1.38 ± 0.05	9.4 ± 0.2
Borated Polyethylene	1.19 ± 0.05	8.8 ± 0.2
Compressed Wood	3.92 ± 0.05	19.0 ± 0.5
Concrete	2.58 ± 0.05	25.0 ± 2.0
Borated Concrete	1.65 ± 0.10	17.5 ± 0.5
Lead	3.00 ± 0.10	26.0 ± 2.0

*0.02 in. cadmium sheet inserted at the interface between the variable core and polyethylene.

**0.02 in. cadmium sheet inserted at both polyethylene-core interfaces.

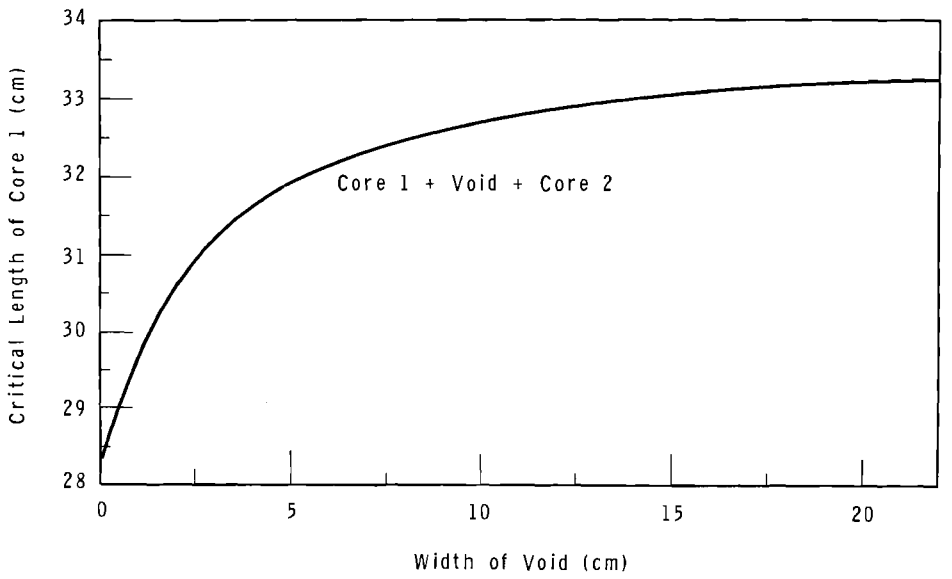

FIGURE 10

Void as Isolator

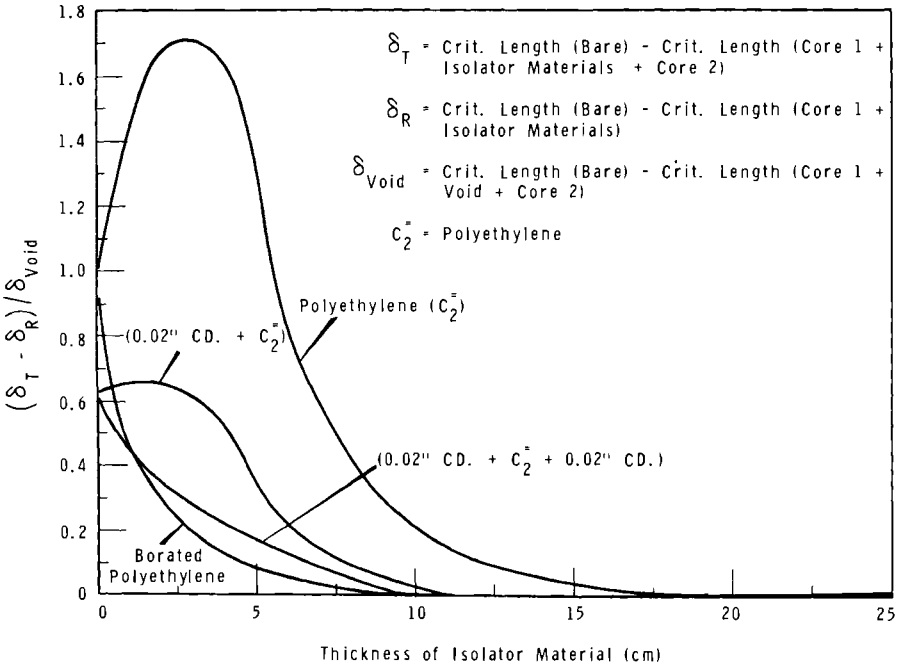

FIGURE 11

Isolating Effect of Various Materials

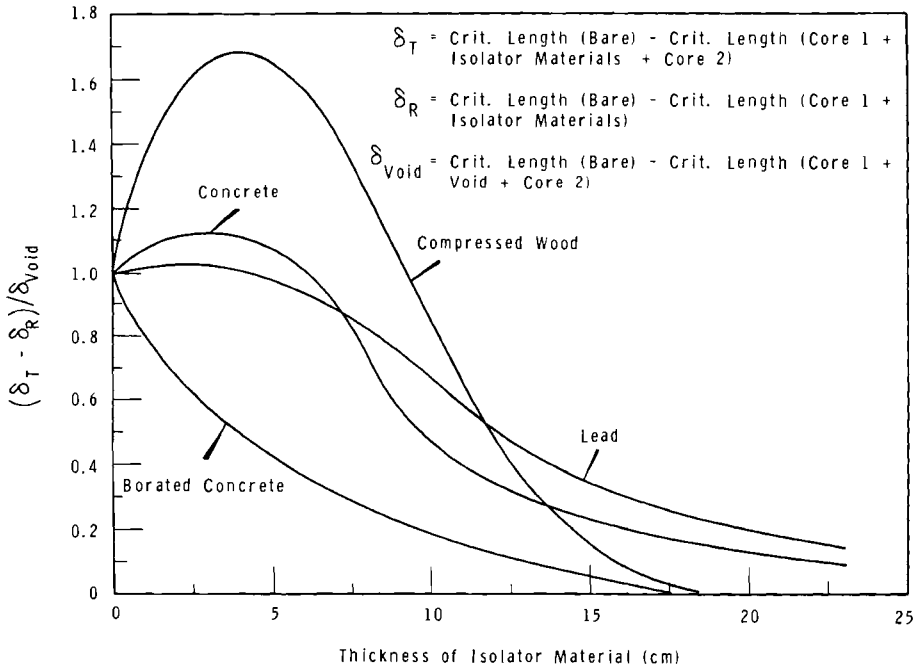

FIGURE 12

Isolating Effect of Various Materials

$(\delta_T - \delta_R)/\delta_{void}$ is plotted as a function of isolator thickness, where

δ_T = L_c (Bare) - L_c (Core 1 + Isolator + Core 2)

δ_R = L_c (Bare) - L_c (Core 1 + Isolator)

δ_{void} = L_c (Bare) - L_c (Core 1 + Void + Core 2)

and

L_c = Critical Length of Core 1.

The corresponding curves for polyethylene and compressed wood have large maximums at 3 and 4 cm respectively; concrete, lead, and polyethylene-0.02 in.-Cd also have maximums, but of smaller magnitude. Although fewer neutrons interact between fuel cores with the isolators located in between, may of the interacting neutrons are moderated by the isolating material which increases their worth in the epithermal fuel cores. Also, $(\delta_T - \delta_R)/\delta_{void} = 0$ is a more sensitive measure of the effective isolation thickness than defined by the asymptotic values in Figures 3 through 10.

References

1. C. R. Richey, E. D. Clayton, R. H. Odegaarden, J. D. White, and W. A. Reardon. Hazards Summary Report for the Hanford Plutonium Critical Mass Laboratory, Supplement No. 1: The Remote Split Table Machine, HW-66266 SUP 1 REV (General Electric Company, Richland Washington). October, 1963.

2. C. R. Richey, J. D. White, E. D. Clayton, S. R. Bierman, K. L. Garlid, and D. R. Skeen. "Critical Experiments with PuO_2-Polystyrene Compacts," Physics Research Quarterly Report, July, August, September, 1963, HW-79054, p. 54 (General Electric Company, Richland, Washington). October 15, 1963.

ONSITE DISTRIBUTION

Copy Number	Pacific Northwest Laboratory
1	D. G. Albertson
2	C. A. Bennett
3	C. L. Bennett
4	R. A. Bennett
5	S. R. Bierman
6	C. L. Brown
7	W. W. Brown
8	S. H. Bush
9	G. J. Busselman
10	J. J. Cadwell
11	J. L. Carter
12	L. L. Carter
13	D. E. Christensen
14	R. G. Clark
15	E. D. Clayton
16	R. E. Dahl
17	L. C. Davenport
18	F. G. Dawson
19	D. R. deHalas
20	R. F. Dickerson
21	B. H. Duane
22	G. W. R. Endres
23	E. A. Eschbach
24	S. L. Fawcett
25	J. R. Fishbaugher
26	D. G. Foster
27	W. E. Foust
28	H. A. Fowler
29	G. C. Fullmer
30	J. J. Fuquay
31	A. G. Gibbs
32	D. W. Glasgow
33	J. Greenborg
34	V. W. Gustafson
35	C. E. Haines
36	R. W. Hardie
37	O. K. Harling
38	R. A. Harris
39	H. Harty
40	R. A. Harvey
41	C. M. Heeb
42	R. E. Heineman
43	H. L. Henry
44	N. A. Hill
45	R. J. Hoch
46	P. L. Hofmann
47	R. H. Holeman
48	R. M. Humes

49 U. P. Jenquin
50 R. L. Junkins
51 E. L. Kelley, Jr.
52 D. A. Kottwitz
53 J. W. Kutcher
54 C. R. Lagergren
55 D. D. Lanning
56 J. H. Lauby
57 B. R. Leonard, Jr.
58 W. R. Lewis
59 R. C. Liikala
60 C. W. Lindenmeier
61 W. W. Little
62 R. C. Lloyd
63 L. L. Maas
64 D. R. Marr
65 R. P. Matsen
66 D. D. Matsumoto
67 R. E. Nightingale
68 L. J. Page
69 H. M. Parker
70 R. S. Paul
71 R. E. Peterson
72 W. W. Porath
73 W. A. Reardon
74 J. J. Regimbal
75 C. R. Richey
76 W. C. Roesch
77 J. T. Russell
78 R. E. Schenter
78 J. E. Schlosser
80 L. C. Schmid
81 D. R. Skeen
82 J. D. Smith
83 R. B. Smith
84 R. I. Smith
85 K. B. Stewart
86 W. P. Stinson
87 J. J. Stoffels
88 D. H. Thomsen
89 C. R. Tipton, Jr.
90 V. O. Uotinen
91 E. E. Voiland
92 M. T. Walling, Jr.
93 J. D. White
94 O. J. Wick
95 R. D. Widrig
96 L. D. Williams
97 J. R. Worden
98 D. C. Worlton

99	H. S. Zwibel
100	Technical Publications
101 - 105	Technical Information Files
106 - 110	Extra (Reactor Physics Section)
	General Electric Company
111	T. W. Ambrose
112	O. F. Beaulieu
113	E. Z. Block
114	C. E. Bowers
115	D. W. Constable
116	R. L. Dickeman
117	R. O. Gumprecht
118	M. M. Hendrickson
119	O. F. Hill
120	H. H. Hopkins
121	G. R. Kiel
122	M. C. Leverett
123	L. M. Loeb
124	W. S. Nechodom
125	R. Nilson
126	D. R. Oden, Jr.
127	G. F. Owsley
128	E. D. Sayre
129	R. J. Shields
130	R. J. Sloat
131	A. E. Smith
132	R. E. Tomlinson
133	R. E. Trumble
	Richland Operations Office
134	M. J. Corrothers
135	J. T. Christy
136	C. D. Compton
137	G. R. Gallager
138	A. T. Gifford
139	P. G. Holsted
140	H. A. House
141	L. R. Lucas
142	R. L. Plum
143	R. G. Rader
144	M. J. Rasmussen
145	M. R. Schneller
146 - 147	R. K. Sharp
148	Technical Information Library

OFFSITE DISTRIBUTION (Special)

Number of Copies	
4	Argonne National Laboratory Reactor Physics Constants Center
11	Atomic Energy Commission, Washington Attn: Assistant Director for Civilian Reactors, DRD (1) F. P. Baranowski, Director Division of Production (1) Chief, Reactor Physics Branch (1) H. Honeck, Reactor Physics Branch(1) K. G. Kolstad, Assistant Director for Physics and Mathematics Programs (1) C. D. Luke, Division of Licensing and Regulations (1) R. J. Odengaarden, Division of Licensing and Regulations (1) J. L. Schwennesen, Assistant Director, Reactor Products, Division of Production (1) E. E. Sinclair, Assistant Director for Advanced Reactor Technology (1) Water Reactor Branch, DRD (2)
1	California Institute of Technology Attn: H. Lurie, Engineering Division
2	Cornell University, Ithaca, N.Y. Attn: R. T. Cuykendall, Engineering Physics R. R. Witson, Physics Department
2	Duke University, Durham, N.C. Attn: H. W. Newson, Physics Department W. J. Seeley, School of Engineering
1	Institute of Atomic Physics Applied Radioactivity Laboratory Bucuresti, CP 35, Rumania Attn: Ing. E. Gaspar
1	Japan Atomic Energy Research Institute (JAERI) Tokai-mura, Naka-gun, Ibaraki-ken, Japan Attn: Hjime Sakata
1	Kansas State University, Manhattan, Kansas Attn: W. R. Kimel, Nuclear Engineering
1	Manhattan College, Riverdale, New York, N.Y. Attn: Brother Gabriel Kane
1	Massachusetts Institute of Technology Attn: Prof. Irving Kaplan
1	New York University Attn: Lyle Borst, Physics Department
1	North Carolina State College Attn: R. L. Murray

ONSITE DISTRIBUTION (Special)

Number of Copies	
1	Purdue University Attn: P. N. Powers, Nuclear Engineering Department
1	Savannah River Operations Office Attn: Robert Thorne
1	Union Carbide Corporation (ORNL) Attn: C. A. Preskitt
1	University of Arizona, Tucson, Arizona Attn: Monte V. Davis, Nuclear Engineering Dept.
1	University of Florida, Gainesville, Florida Attn: R. E. Uhrig, Nuclear Engineering
1	University of Illinois, Urbana, Illinois Attn: Frederick Seitz, Physics Department
1	University of Michigan, Ann Arbor, Michigan Attn: J. H. Gomberg, Nuclear Engineering Dept.
1	University of Minnesota, Minneapolis, Minnesota Attn: H. S. Isben, Chemical Engineering Dept.
1	University of Nevada, Reno, Nevada Attn: T. V. Frazier, Physics Dept.
1	University of Notre Dame, Notre Dame, Indiana Attn: E. W. Jerger, Department of Mechanical Engineering
1	University of Oregon, Eugene, Oregon Attn: J. L. Powell, Physics Department
2	University of Tennessee, Knoxville, Tennessee Attn: A. H. Nielsen, Physics Dept. P. F. Pasqua, Nuclear Engineering Dept.
1	University of Toledo, Toledo, Ohio Attn: J. J. Turin
1	University of Washington, Seattle, Washington Attn: A. L. Babb, Dept. of Nuclear Engineering
1	University of Wisconsin, Madison 6, Wisconsin Attn: M. W. Carbon, Nuclear Engineering Committee
1	Virginia Polytechnic Institute, Blacksburg, Virginia Attn: Andrew Robeson, Physics Dept.
1	Washington State University, Pullman, Washington Attn: J. P. Spielman, College of Engineering
1	United Nuclear Corp., White Plains, New York Attn: George Sofer